

Evidence for the brown carbon absorption over the Bay of Bengal during the southwest monsoon season: a possible oceanic source

Poonam Bikkina^{1,*}, Srinivas Bikkina², Kimitaka Kawamura², A.K. Sudheer³, G. Mahesh³, and S. Kuswanth Kumar^{1,4}

¹National Institute of Oceanography, Regional Centre Waltair, Visakhapatnam, Andhra Pradesh 530017, India

²Chubu Institute for Advanced Studies, Chubu University, Kasugai, Aichi, 487-8501, Japan

³Geosciences Division, Physical Research Laboratory, Ahmedabad, India

⁴University of Hyderabad, Hyderabad 500 046, Telangana State, India

Revision submitted to

“Environmental Science: Process and Impacts”

23 June 2020

***Corresponding author**

Poonam Bikkina (E-mail: ptyagi@nio.org)

Short Title: BrC in pristine marine aerosols of BoB

Abstract

The near UV-visible light-absorbing organic carbon (OC) of ambient aerosols, referred here as brown carbon (BrC), significantly influence the atmospheric radiative forcing on both regional and global scales. Here, we documented BrC absorption in the aqueous and methanol extracts of marine aerosols collected over the Bay of Bengal (BoB: September-October 2017) and a city, Visakhapatnam (May-June 2018) in southern India during the southwest monsoon (i.e., a transition period with weak continental impact). The absorption spectra of BrC over the BoB showed several peaks around 300-400 nm and differ from those observed over Visakhapatnam. The absorption coefficient of BrC over the BoB, unlike Visakhapatnam data, does not seem to covary with other chemical proxies of biomass burning (non-sea-salt or nss-K⁺) and coal combustion (nss-SO₄²⁻) in the continental outflows, suggesting a different source of BrC over the BoB. Besides, we observed higher proportions of water-insoluble organic carbon (WIOC/OC: 0.89±0.02) and significant enrichment of Mg²⁺ over Na⁺ (i.e., relative to seawater) in BoB aerosols. This result, and the backward air mass trajectories, both hinted their major source of OC from marine-derived organic matter. In contrast, the absorption spectra of BrC over Visakhapatnam are like those from biomass burning emissions in the Indo-Gangetic Plain. This observation is further supported by the satellite-based fire counts and backward air mass trajectories. Therefore, our study underscores the BrC aerosols from the oceanic sources and southern India, hitherto unknown and can improve our understanding of the regional climate effects of carbonaceous aerosols if included in models.

Words: 229

Keywords: BrC-like light-absorbing compounds, Bay of Bengal, Visakhapatnam, southwest monsoon, marine aerosols.

Graphic Art:

1. Introduction

Light-absorbing organic aerosols (*aka.* brown carbon: BrC) have recently gained considerable attention among the scientific peers due to their potential influence on both regional and global climate via direct (*i.e.* by their absorbing nature) and indirect effects (*i.e.* evaporating the clouds once dissolved and, thus, affecting cloud lifetime)¹⁻⁴. BrC includes a class of organic compounds present in the ambient air, which show prominent UV-visible light absorption (*i.e.* between 300-700 nm)⁵⁻⁷. These aerosols can be directly emitted from incomplete combustion of fossil fuels, industrial processes, domestic heating, and biomass burning⁸⁻¹¹ and secondarily formed by the oxidation of volatile organic compounds of anthropogenic and biogenic origins¹²⁻¹⁷. Primary and secondary aerosols from biomass burning emissions are shown to be a major source of BrC on regional and global scales^{6, 15, 18-21}. Humic-like substances (HULIS) account for an important fraction of primary BrC¹⁵. Their optical properties depend on various atmospheric processes (*e.g.*, chemical reactions, changes in solar irradiation and relative humidity)²²⁻²⁴, which make the identification of individual BrC species very difficult.

Despite the ubiquitous occurrence of BrC aerosols, there is a growing interest to study their sources, absorption characteristics, and transformations in detail over South and East Asia due to the ongoing increase in anthropogenic activities (*e.g.*, biomass burning, fossil fuel combustion)^{7, 25, 26}. To this date, studies focusing on BrC aerosols over South Asia are, in particular, limited to the Indo-Gangetic Plain (IGP) and its outflow to the Bay of Bengal (BoB) and the northern Indian Ocean (NIO) during the early and late northeast monsoon (December – April)^{20, 27-34}. These studies have mostly attributed the sources of BrC aerosols to postharvest crop-residue burning emissions in the northwest IGP (*e.g.*, Punjab and Haryana). However, the BoB and NIO witness the impact of continental outflow mostly from the IGP, but with some contribution from coastal cities in the southern part of the Indian peninsula^{35, 36}. Recent studies have documented the presence of coloured dissolved organic matter (*aka.* CDOM) in the surface waters of the BoB and these compounds have a near UV-visible absorption between 300 nm and 600 nm similar to that of continental BrC^{37, 38}.

The oceanic CDOM can be incorporated into the sea salt aerosols and can be reinforced by the strong seasonal winds over the BoB, where their contribution could affect the overall absorption properties and radiative forcing of carbonaceous aerosols in the marine atmosphere. However, studies documenting the presence of marine-derived BrC over the BoB is so far lacking in the literature. In this study, our major goal was to ascertain whether such ocean-derived BrC contributes to atmospheric aerosols collected over the BoB and a coastal city, Visakhapatnam during the southwest monsoon. Furthermore, the absorption spectra of BrC and other associated optical

properties from this study were compared with those typically observed for the wintertime aerosols from the BoB and the CDOM data from the estuarine waters draining into the BoB.

2. Materials and methods

2.1. Site description and prevailing meteorology

The BoB is one of the two limbs of the NIO and is located on the eastern side of peninsular India. During the southwest monsoon, the BoB receives immense freshwater supply from mighty rivers such as Ganga and Brahmaputra. Consequently, a large amount of terrigenous particulate matter from these rivers, strong stratification of freshwater, intense cloud cover during the southwest monsoon season make the BoB poorly ventilated and, thus, contribute to low primary productivity^{39, 40}. In contrast, the cyclonic eddies often bring nutrient-rich subsurface waters to the sunlit surface ocean during spring (April-May) and fall seasons (September-October) and, thus, thrive phytoplankton productivity^{41, 42}. Additionally, the BoB experiences a seasonal reversal of prevailing meteorology between winter/spring and summer/fall seasons. The continental outflow from the IGP acts like a conduit of air pollutants (and BrC) to the marine atmosphere of BoB during the northeast monsoon (predominantly in winter)^{25-27, 29}. In contrast, winds blow mostly from the ocean to land during the southwest monsoon season, and, hence, we could expect a lesser influence from the anthropogenic emissions (or BrC) over the BoB^{27, 43}.

Recent studies have documented the abundance of CDOM in the coastal and offshore waters of the BoB^{37, 38}. In such a case, CDOM could be emitted along with sea-spray aerosols and, hence, contributes to the absorption of carbonaceous aerosols over the BoB. Therefore, we focused on whether there exists any such *BrC-like* material in the marine atmospheric boundary layer of the BoB during the southwest monsoon. This is achieved by looking at the BrC absorption signals in two sets of PM₁₀ aerosols (*i.e.* aerodynamic diameter $\leq 10 \mu\text{m}$) (i) those collected onboard research vessel Sindhu Sankalp during the cruise in the BoB (SSK105: 23 September to 4 October 2017) and, (ii) from a coastal urban location, Visakhapatnam in Southern India (Figure 1a).

2.2. Aerosol collection and analysis of WSOC

We collected eight PM₁₀ samples from the BoB along with three field blanks on precombusted Tissuquartz filters (PALLFLEX[®]TM, baked at 450 °C for 8h) from 23 September to 4 October 2017. The PM₁₀ air sampler (Envirotech, flowrate $\approx 1.0 \text{ m}^3 \text{ min}^{-1}$) was installed on the front deck of the research vessel, Sindhu Sankalp to avoid any potential contamination from the ship's exhaust and was operated only when the ship speed was more than 10-12 knots h^{-1} . The SSK105 cruise was conducted in offshore waters of the BoB and more details regarding the sampling times

and other information are provided in Table S1. Nine PM₁₀ samples were also collected using the same PM₁₀ air sampler that was set upon the rooftop of the five-storey building (~20m above msl) of National Institute of Oceanography regional center (NIORC) in Visakhapatnam (Figure 1a) from 16 May to 4 June 2018. Of these, the first two filter samples were collected as pilot runs to see whether we could detect any meaningful BrC absorption signal or not by using a 24 and 12 h integrated high-volume aerosol samples during summertime over Visakhapatnam. After looking at the absorption spectrum of BrC from these aerosol filters, we decided to collect aerosol samples only during nighttime to avoid or minimize the influences from local traffic. All other PM₁₀ samples from Visakhapatnam were collected mostly during nighttime (18:00-06:00; Table S2) when the airmasses blow from the oceanic region (sea breeze).

After collection, aerosol filters were sealed in airtight Ziploc bags and stored at -20 °C until further analysis. For the measurement of water-soluble organic carbon (WSOC), ~10.05 cm² area of the filter cut was extracted with ultrapure deionized water (Milli-Q; specific resistivity >18.2 MΩ-cm). The extract was subsequently filtered using a pre-cleaned 10 ml glass syringe connected to a disc filter (Millex-GV, 0.22 μm) and the filtrate was injected to a total organic carbon analyzer (Model TOC-Vcsh, Shimadzu) for the determination of WSOC as non-purgeable organic carbon (NPOC). In the TOC analyzer, the dissolved organic carbon is catalytically oxidized under high temperature to CO₂, which is quantified by a non-dispersive infrared detector (NDIR). The TOC instrument was calibrated using the gravimetrically prepared potassium hydrogen phthalate standard dilutions⁴⁴.

2.3. Absorption properties of BrC

A portion of PM₁₀ sample (~45 mm dia.) was extracted with ~35 ml of organic free ultrapure deionized water. Likewise, ~4-6 circular filter punches of PM₁₀ samples (~20 mm dia.) were extracted with ~25 ml methanol in pre-combusted glass tubes using ultrasonic agitation (10 min × 3 times). These solvent extracts were centrifuged and filtered through a 0.7 μm Whatman GF/F filter and the absorption spectra were recorded between 200 and 700 nm using the UV-visible spectrometer (Shimadzu UV-Vis 1800 model). However, we only showed the absorption spectra from 300 nm to 700 nm to consistently compare with the literature measurements. The absorbance of water- and methanol-extracts at 365 nm relative to 700 nm are used to estimate the absorption coefficient of water- and methanol-soluble BrC ($b_{abs-H_2O/MeOH-BrC-365nm}$; expressed in Mm⁻¹; M = 10⁶)^{27, 45}.

$$b_{abs-H_2O/MeOH-BrC-365nm} (Mm^{-1}) = \frac{(A_{365nm} - A_{700nm}) * V_{extract} * \ln(10)}{(V_{air} * l)} \quad (1)$$

In Eqn 1, $A_{365 \text{ nm}}$ and $A_{700 \text{ nm}}$ correspond to measured absorbances at 365 nm and 700 nm, respectively. V_{extract} refers to the volume of organic free ultrapure deionized water or organic solvent used for extraction and V_{air} is the volume of air filtered (expressed in m^3), respectively. Likewise, l is the path length of cell (*i.e.* 1 cm) used for light absorption measurement. Although the entire absorption spectrum between 300 nm and 700 nm were obtained, we only used 365nm to quantify the $b_{\text{abs-H}_2\text{O/MeOH-BrC-365 nm}}$ to compare our results with the existing literature on BrC studies over South Asia and elsewhere. This implies that $b_{\text{abs-BrC}}$ can be computed for other wavelengths also. The $b_{\text{abs-H}_2\text{O/MeOH-BrC}}$ values are somewhat dependent on wavelength in a power relation (Eqn 2) and, the power exponent is referred as “absorption Ångström exponent (AAE_{BrC})”^{6, 7, 10, 34, 46-48}.

$$b_{\text{abs-H}_2\text{O/MeOH-BrC}-\lambda} (M m^{-1}) \propto \lambda^{-AAE_{\text{BrC}}} \quad (2)$$

The $b_{\text{abs-H}_2\text{O-BrC-365nm}}$ is normalized with the mass concentration of WSOC would provide mass absorption efficiency ($MAE_{\text{BrC-365 nm}}$, in units of $\text{m}^2 \text{g}^{-1}$).

$$MAE_{\text{H}_2\text{O-BrC-365 nm}} (\text{m}^2 \text{g}^{-1}) = \frac{b_{\text{abs-H}_2\text{O-BrC-365 nm}} (M m^{-1})}{WSOC (\mu\text{g m}^{-3})}$$

$$(3) MAE_{\text{MeOH-BrC-365 nm}} (\text{m}^2 \text{g}^{-1}) = \frac{b_{\text{abs-BrC-365 nm}} (M m^{-1})}{OC (\mu\text{g m}^{-3})} \quad (4)$$

For this study, we have also measured the absorption spectra of solvent blanks (*i.e.*, Milli-Q water and methanol) before measuring the aerosol extracts for BrC-absorption. No measurable absorption was found for the solvent blanks. The solvent extract-based BrC absorption properties are not directly representative of their particle characteristics in the ambient atmosphere. Hence, we cannot directly compare the absorption coefficient and mass absorption efficiency of water- or methanol-soluble BrC in ambient aerosols with that of other strongly absorbing particulate elemental carbon (EC)⁶. It is, therefore, a prerequisite to translate or convert the solvent extractable BrC optical properties to their ambient aerosol particles⁶. For the Rayleigh regime (*i.e.* for small particles), Sun *et al.*⁴⁹ have suggested a conversion factor (ξ) ≈ 0.7 where the size parameter of aerosols is far less than one (*i.e.* $\pi d/\lambda \ll 1$; d = particle diameter). Alternatively, Liu *et al.*⁵⁰ compared the Mie theory-based MAE_{BrC} in the particulate phase with bulk solution derived BrC absorption properties and found that the latter approach (*i.e.* solvent-extractable BrC) significantly underestimates the MAE_{BrC} by a factor of two. Given the broad disparity between these studies, direct use of either of these conversion factors for upscaling/downscaling the measured BrC absorption from the solvent extract would affect reciprocally and may not alter the interpretations in this study. Accordingly, we have not scaled our MAE_{BrC} values based on the water- and methanol-extracts (*i.e.* according to Eqn 5, where $\xi \approx 1$; for this study), but instead directly compared with MAE_{EC} to estimate the imaginary

component of the refractive index of BrC as well as relative radiative forcing efficiency of BrC over EC (see section 3.5).

$$MAC_{aero-BrC}(\lambda) = \xi \times MAE_{BrC-MeOH/H_2O}(\lambda) \quad (5)$$

The light-extinction caused by a BrC substance in the atmosphere can be well described by the complex refractive index ($\mu \approx m+ik$), where the real (m) and imaginary (k) parts refer to scattering and absorbing effects, respectively^{49, 51, 52}. The MAE of BrC at a measured wavelength ($\lambda = 365$ nm) from methanol and water-extracts of PM₁₀ samples can, thus, be translated to estimate their imaginary refractive index of BrC according to Eqns 6 and 7⁵⁰.

$$k_{BrC-MeOH-\lambda} = \frac{(MAE_{MeOH-BrC-\lambda})\rho\lambda}{4\pi} \quad (6)$$

$$k_{BrC-H_2O-\lambda} = \frac{(MAE_{H_2O-BrC-\lambda})\rho\lambda}{4\pi} \quad (7)$$

Here, ‘ ρ ’ is the density of BrC aerosols (expressed in g. cm⁻³). Sumlin *et al.*⁵³ reported ‘ ρ ’ values between 0.8 and 1.2 g cm⁻³ for the biomass burning derived BrC particles. Rissler *et al.*⁵⁴ estimated the particle density of light-absorbing OC in an urban atmosphere as 1.4 g cm⁻³. Likewise, Mok *et al.*⁵⁵ have used a particle density of 1.2 g cm⁻³ for assessing the impact of BrC absorption from the Amazonian biomass burning emissions on surface UV and ozone photochemistry. Reid *et al.*⁵⁶ have compiled the density of smoke particles (1.2-1.4 g cm⁻³) emitted from the biomass burning emissions. In contrast, Shamjad *et al.*³² have used a somewhat higher value of particle density of organic carbon 1.5 g cm⁻³ for assessing the k_{BrC} over the central IGP. Given the broad range of particle density values for the light-absorbing OC in the literature, we, therefore, used a ‘ ρ ’ value of BrC aerosols (1.4±0.1 g cm⁻³) for assessing the k_{BrC} .

2.4. Carbonaceous species -mass absorption efficiency of elemental carbon (EC)

We analyzed the mass concentrations of elemental carbon (EC) and organic carbon (OC) in PM₁₀ samples using thermo-optical transmittance (TOT) method on a semi-continuous Sunset carbon analyzer (*i.e.* operated in offline mode) at Chubu University, Japan, according to the procedures described in Miyazaki *et al.*⁵⁷. The accuracy of the semicontinuous analyzer for the total carbon content was periodically assessed (*i.e.* within 10%) by the gravimetrically prepared sucrose and potassium hydrogen phthalate standards. Furthermore, we used the light-absorption data of EC from the semi-continuous Sunset carbon analyzer for the mass absorption efficiency (MAE) of EC according to the analytical protocol described by Ram and Sarin⁵⁸. Briefly, the laser transmission signal (here $\lambda = 660$ nm) from the Sunset carbon analyzer (or attenuation, ATN) can be used to estimate the MAE of EC using the following mathematical expressions.

$$b_{\text{ATN-EC-660}} (\text{Mm}^{-1}) = \text{ATN}_{\text{EC-660}} \times A_{\text{filter}} / V_{\text{air}} \quad (8)$$

$$b_{\text{abs-EC-660}} (\text{Mm}^{-1}) = b_{\text{ATN-EC-660}} (\text{Mm}^{-1}) / [C \times R(\text{ATN})] \quad (9)$$

where $b_{\text{ATN-EC-660}}$ and $b_{\text{abs-EC-660}}$ are the attenuation and absorption coefficients, respectively and $M=10^6 \cdot V_{\text{air}}$ is the volume of air sampled (*i.e.* expressed in m^3) through a filter (A_{filter} : $\sim 405 \text{ cm}^2$). To obtain the $b_{\text{abs-EC-660}}$, $b_{\text{ATN-EC-660}}$ needs to be corrected for the filter loading effect ($R(\text{ATN})$) and the multiple scattering effect (C), respectively. $R(\text{ATN})$ is based on the empirical relations initially suggested by Weingartner *et al.*⁵⁹ for the Aethalometer and later used by Ram and Sarin⁵⁸ for assessing the MAE_{EC} based on the light attenuation and mass concentration of EC⁵⁸. The parameter C is due to lensing effect of sulfate and organics on EC as this causes enhancement in the absorption, whereas $R(\text{ATN})$ is the reduction in absorption of EC embedded in the filter depths across the light path of the aerosol filter. Ram and Sarin⁵⁸ have suggested a ‘ C ’ value between 2.1 and 5.0 for the externally and internally mixed type of EC, respectively. As samples were collected from the distant locations and also, EC is likely a mixture of both internally/externally mixed types, we chose an intermediate value of 3.6 for the C . Besides, $R(\text{ATN})$ is calculated based on the following mathematic expression.

$$R(\text{ATN}) = \left(\frac{1}{f} - 1 \right) \left[\frac{\ln(\text{ATN}) - \ln(10\%)}{\ln(50\%) - \ln(10\%)} \right] + 1 \quad (10)$$

Weingartner *et al.*⁵⁹ have proposed to use an ‘ f ’ value of 1.103 and 1.14 for the presence of internally and externally mixed EC aerosols. For this study, we used an ‘ f ’ value of 1.103 for the samples with ATN more than 10% (*i.e.*, because aerosols collected over the BoB) and ‘ f ’ ≈ 1 for ATN $< 10\%$ ⁵⁸. We estimated the $\text{MAE}_{\text{EC-660}}$ by normalizing the $b_{\text{abs-EC-660}}$ with the mass concentration of EC (in $\mu\text{g m}^{-3}$) as described in Eqn 11 given below.

$$\text{MAE}_{\text{EC-660}} (\text{m}^2 \text{ g}^{-1}) = b_{\text{abs-EC-660}} (\text{Mm}^{-1}) / [\text{EC} (\mu\text{g m}^{-3})] \quad (11)$$

Uncertainty analysis was also conducted for the optical properties of BrC based on the Montecarlo simulation of error propagation (MCEP). For this, we used the external precision of absorbance ($< 20\%$), air volume filtered ($< 3\%$), WSOC and OC concentrations ($< 10\%$) as errors in the MCEP-based calculation of $b_{\text{abs-H}_2\text{O/MeOH-BrC-365 nm}}$, $\text{MAE}_{\text{H}_2\text{O/MeOH-BrC-365 nm}}$ and $k_{\text{BrC-H}_2\text{O/MeOH}}$ (Table S3).

3. Results and discussion

3.1. Backward air mass trajectory analysis

The air mass backward trajectory analysis provides crucial information about the likely contribution of source-emissions to BrC aerosols collected over the BoB and Visakhapatnam. We computed 7-day isentropic air mass backward trajectories (BTs) for the sampling days at the midpoint of cruise tracks using archived meteorological data sets from NOAA air resources laboratory on a PC-based hybrid single particle lagrangian integrated trajectory model (HYSPLIT, version 4.0)⁶⁰. The BTs were computed at 100 m above sea level during SSK105 the cruise mostly showed marine origin (Figure 1b; *i.e.* from the NIO), indicating the likely influence of organic matter associated with seasalt aerosols. It is also worth mentioning that the height of BTs for the PM₁₀ samples collected during SSK105 cruise when passing over southern India was increased to ~500 – 1500 m (Figure S1) and, hence, less likely influenced by the ground-level emissions of biomass burning (BB). Likewise, the 7-day isentropic air mass BTs over Visakhapatnam showed a mixed influence of oceanic and continental sources (Figure 1c), in particular, originated from the northwestern IGP. Coincidentally, the sampling period overlaps with the occurrence of postharvest crop-residue burning emissions (*e.g.*, wheat-crop-residue: late April-early May) over the IGP. Therefore, we have examined the moderate resolution imaging spectroradiometer (MODIS) satellite-based firecount data for the sampling period (Figure 1d). Combining the BTs and MODIS firecounts, we could expect that aerosols over Visakhapatnam during May-June 2018 have been influenced by the wheat residue burning emissions in the IGP. Therefore, the observed BrC aerosol absorption over Visakhapatnam (if any) could likely be contributed from this open biomass burning events.

3.2. Absorption spectra of BrC-relationship with chemical tracers

The absorption coefficient of BrC at 365 nm assessed from the water and methanol extracts of aerosols ($b_{abs-BrC-H_2O-365\text{ nm}}$ and $b_{abs-BrC-MeOH-365\text{ nm}}$) collected over the BoB was lower than that observed over Visakhapatnam (Table 1). This implies that PM₁₀ samples from Visakhapatnam have abundant and different chromophores than those from the BoB. Besides, the absorption coefficient of water/methanol-soluble BrC over the BoB (Figure 2a-b) showed several peaks across the measured wavelength range (300-700nm) unlike those observed over Visakhapatnam (Figure 2c-d). This observation also suggests a likely difference in contributing sources of BrC aerosols between the BoB and Visakhapatnam. This argument is further strengthened by the similarity in the wavelength-dependent absorption spectra of BrC from Visakhapatnam with the biomass burning influenced aerosols from the IGP/IGP-outflow (Figure S2)^{25,61}. Coincidentally, air mass BTs, MODIS-VIIRS fire

count and absorption spectra of BrC altogether over Visakhapatnam suggest a contribution from biomass burning emissions.

In this study, we noticed that BrC absorption from methanol extracts in most of the PM₁₀ samples over both geographical domains was lower than the aqueous extracts (Figure 3). This feature is in sharp contrast to those documented from the wintertime biomass burning emissions in the IGP in South Asia^{61, 62} as well as those reported for anthropogenic emissions (*e.g.*, biomass burning and fossil-fuel combustion) over other parts of East Asia⁶³⁻⁶⁷. Mostly, studies focusing on BrC absorption from the water and methanol extracts of ambient aerosols have only discussed the broad spectral features and emphasized that water-insoluble fraction of BrC is more absorptive in nature. Therefore, the prevailing differences in the BrC absorption from the solvent extracts between this study and those others in the literature could be due to two plausible reasons. First, the BrC aerosols over the BoB during southwest monsoon season could have a contribution from a different source other than the continental pollution (*i.e.*, air mass BTs showed maritime influence) and containing BrC-chromophores that are more soluble in water than methanol. Second, there could be significant photobleaching effects of different constituent chromophores associated with WSOC or WIOC in our summertime PM₁₀ samples.

The $b_{\text{abs-H}_2\text{O-BrC}}$ and $b_{\text{abs-MeOH-BrC}}$ showed significant temporal variability over the BoB and Visakhapatnam (Figure 3). The temporal trends of $b_{\text{abs-H}_2\text{O/MeOH-BrC}}$ over the BoB are not comparable with other chemical tracers of continental outflow including nss-K^+ and nss-SO_4^{2-} (*i.e.* a proxy for the impact of biomass burning and coal combustion, respectively). In contrast, some similarity persists in the temporal variability for the Visakhapatnam data between $b_{\text{abs-H}_2\text{O/MeOH-BrC}}$ and these anthropogenic tracers (Figure 3), suggesting an influence from biomass burning emissions to ambient BrC. As the air mass BTs during SSK105 cruise originated mostly from the Indian Ocean, detectable EC concentration ($0.8\text{-}1.2 \mu\text{g m}^{-3}$) in these samples suggests somewhat a mixed influence of continental and oceanic sources. Several studies from the continental outflows to the BoB and NIO revealed significant positive linear relationships between WSOC and OC with higher slopes > 0.60 ^{58, 68}. This is because of the oxidation of biomass burning organic aerosols from the IGP/SE Asia during long-range transport. Nevertheless, we found no significant linear relationship of WSOC and EC with OC over the BoB. This observation suggests that these carbonaceous components have a different origin other than the continental outflow over the BoB during SSK105 cruise. In contrast, there exist significant linear relationships of WSOC and EC with OC in PM₁₀ sampled over Visakhapatnam together with the air mass trajectories and MODIS-VIIRS fire count data (Figures 1c,d), suggesting their common source-emissions or long-range transport. Therefore, a lack of

similarity in the temporal trends between $b_{\text{abs-H}_2\text{O/MeOH-BrC}}$ and other chemical tracers used here (nss- K^+ , nss- SO_4^{2-} , and OC) during SSK105 cruise altogether indicate the contribution of *BrC-like* substances from non-biomass burning sources.

In the neritic waters, humic substances delivered through peninsular rivers and other major rivers to the BoB also usually absorb light in the near UV-visible region with a monotonous decrease of absorption towards visible wavelength similar to BrC aerosols³⁸. This class of organic compounds in the surface seawater is CDOM. The absorption coefficient of CDOM ($b_{\text{abs-CDOM}}$) usually expressed in m^{-1} and is defined as given below^{38, 69}.

$$b_{\text{abs-CDOM}}(\lambda) = A(\lambda) \times \ln(10)/l \quad (12)$$

Here, $A(\lambda)$ is absorbance measured across the wavelength range of 300-700 nm and ' l ' is the path length of the cell used for the absorption measurement. Recently, Sarma *et al.*⁶⁹ documented the absorption spectra of CDOM (*i.e.* similar to ambient BrC) from the surface seawater samples collected from the mouth of the Gautami-Godavari estuary, which is draining into the BoB, during 6-19 May 2011 (Figure S3). Therefore, *BrC-like* organic compounds could be transported from the surface waters along with the SSAs, contributing to PM_{10} during the inter-monsoon period.

O'Dowd *et al.*⁷⁰ have found that SSAs are largely composed of water-insoluble organic carbon (WIOC) and contain mostly insoluble colloidal aggregates and phytodetritus^{52, 53}. Therefore, if marine-derived organic matter contributes to ambient aerosols, we can expect a much higher fraction of water-insoluble organic carbon (WIOC \approx OC-WSOC) to total OC measured in aerosols. Accordingly, we found high mass ratios of WIOC/OC ($89 \pm 2\%$) in PM_{10} sampled over the BoB during SSK105 cruise (Figure 4). Likewise, organic aerosols influenced by the biological activity in the surface ocean are more enriched with Mg^{2+} relative to Na^+ than in seawater (*i.e.* $(\text{Mg}^{2+}/\text{Na}^+)_{\text{aerosol}} > (\text{Mg}^{2+}/\text{Na}^+)_{\text{seawater}}$)⁷¹⁻⁷³. Here, the $\text{Mg}^{2+}/\text{Na}^+$ ratio in seawater is apparently constant irrespective of the salt content of world oceans. Therefore, we computed the enrichment factor of Mg^{2+} ($\text{EF}_{\text{Mg}^{2+}} = (\text{Mg}^{2+}/\text{Na}^+)_{\text{aerosol}} / (\text{Mg}^{2+}/\text{Na}^+)_{\text{seawater}}$) for the PM_{10} samples from the BoB and Visakhapatnam. Higher $\text{EF}_{\text{Mg}^{2+}}$ values (*i.e.* > 1) over the BoB than Visakhapatnam indicate a greater influence of marine-derived organic aerosols during SSK105 cruise. The riverine supply is a source of humic substances to the seawater and is a significant contributor to WSOC pool. This means we could expect higher values of the absorption coefficient of BrC in the water-extracts than methanol extracts. Consistently, the $b_{\text{abs-H}_2\text{O-BrC}}/b_{\text{abs-MeOH-BrC}}$ ratios (*i.e.* the size of the circles in Figure 4) over the BoB are higher than those observed at Visakhapatnam. This probably means that marine-derived

BrC (*i.e.* CDOM like material) could cause such high $b_{\text{abs-H}_2\text{O-BrC}}/b_{\text{abs-MeOH-BrC}}$ ratios observed over the BoB.

3.3. Comparison of absorption properties

We also compared the absorption properties of water-soluble BrC ($b_{\text{abs-H}_2\text{O-BrC-365nm}}$, $\text{MAE}_{\text{H}_2\text{O-BrC-365nm}}$, and $\text{AAE}_{\text{H}_2\text{O-BrC}}$) from the SSK105 cruise (*i.e.* late southwest monsoon) with the SS259 cruise (*i.e.* northeast monsoon; Figure 5)²⁷. There exists a marked difference in the origin of air masses between these two cruises conducted in the BoB²⁷. The air masses sampled during SSK105 cruise (September-October 2017) are mostly oceanic origin, whereas those collected during SS259 cruise (November 2008) have continental influence²⁷. The $b_{\text{abs-H}_2\text{O-BrC-365 nm}}$ (Figures 5a,b) over the BoB during the southwest monsoon season (this study) is lower by a factor of two than those observed during the continental outflow (*i.e.*, SS259: November 2008). This observation suggests a greater source strength of BrC emissions from the continental sources during SS259 compared to those emitted along with sea salt aerosols during SSK105. Furthermore, the spectra of $b_{\text{abs-H}_2\text{O-BrC-}\lambda}$ over the BoB showed a highly variable peak maximum (Figure 2a) compared to those typically observed monotonous relationships in marine and/or continental aerosols during the northeast monsoon (Figure S2)^{27, 28, 31-33, 74}.

The $\text{MAE}_{\text{H}_2\text{O-BrC-365 nm}}$ is also comparable between both cruises (*i.e.* SSK105 & SS259; Figures 5c, d) as well as to those reported from other studies in the IGP and its outflow to the NIO during the northeast monsoon (Table 2, Figure S2). This observation, thereby, emphasizes an overall considerable influence of *BrC-like* organic matter emitted from the BoB during the southwest monsoon. Here the comparable $\text{MAE}_{\text{H}_2\text{O-BrC-365nm}}$ values between southwest monsoon season (this study) and the winter cruise (SS259) are likely because of the distinct and characteristic BrC-absorption signal of the WSOC fraction between two source emissions (marine and continental). The marine-derived organic matter associated with sea salt aerosols containing less BrC-absorption and lower WSOC than those influenced by the wintertime continental outflow to the BoB.

The AAE values obtained from the wavelength dependence of BrC absorption ($b_{\text{abs-BrC}} \propto \lambda^{-\text{AAE}}$) in ambient aerosols provide useful information about their contributing sources⁷⁵⁻⁷⁷. From the absorption spectra of water- and/or methanol-soluble BrC data from SSK105 and Visakhapatnam, we, therefore, deduced $\text{AAE}_{\text{H}_2\text{O/MeOH-BrC}}$ based on the linear regressions between $\log \lambda$ and $\log(b_{\text{abs-H}_2\text{O/MeOH-BrC-}\lambda})$. We observed significant differences in the AAE_{BrC} values between the southwest monsoon (SSK105: 3.1 ± 1.1) and northeast monsoon cruise datasets (SS259: 5.8 ± 1.5) from the BoB, possibly related to compositional differences in the water-soluble BrC chromophores

(Figures 5e, f). Organic compounds containing conjugated double bonds (or aromatic character) and substituted with electron-donating (*e.g.*, -OH, -NH₂) or electron-withdrawing functional groups (*e.g.*, -NO₂, -COOH), absorb towards longer wavelengths besides near UV-visible region and, thus, can have lower AAE_{BrC}^{78, 79}. Because of the prevailing maritime air masses and lack of correlations between anthropogenic tracers (nss-K⁺, nss-SO₄²⁻, OC, WSOC and EC) and $b_{\text{abs-H2O-BrC-365nm}}$ during the SSK-105 cruise (this study), the BrC aerosols could have originated from the organic matter associated with seasalt aerosols (Figure 3e). In contrast, the rapid photobleaching of BrC-chromophores during the wintertime continental outflow to the BoB (ageing effect) could weaken the visible absorption and result in increased AAE²⁶ (*i.e.*, the case for SS259 cruise; Figure 3f).

3.4. Relationship between the refractive index of BrC and EC/organic matter

The imaginary component of the refractive index of BrC (k_{BrC}) is a key input to global climate model for predicting the radiative impacts of organic aerosols^{8, 15, 32}. Based on the controlled laboratory combustion of several wild fuels, Saleh *et al.*¹ have proposed that the BrC-absorption is strongly linked with EC content in aerosols emitted from the biomass burning. Furthermore, Saleh *et al.*¹ have shown that k_{BrC} positively correlated with the mass ratio of EC to organic matter (OM). In this study, the air mass BTs and MODIS fire count data over Visakhapatnam hinted the influence of wheat-crop residue burning emissions in the IGP (Figures 1c, d). Therefore, we looked for any such prevailing positive covariability between $k_{\text{BrC-365nm}}$ and EC/OM (here $\text{OM} \approx \text{OC} \times 1.4^{\text{80, 81}}$). However, we could not observe any significant relationship between $k_{\text{BrC-MeOH/H2O-}\lambda}$ and EC/OM (Figure 6). Our findings are consistent with similar reports from the IGP and the IGP-outflow to the Indian Ocean during the northeast monsoon in terms of lack of relationship between $k_{\text{BrC-MeOH/H2O-}\lambda}$ and EC/OM^{25, 74}. This observation, therefore, warrants a further investigation on controlling factors that change the optical properties of ambient BrC, *e.g.*, photochemical ageing processes occurring in the atmosphere.

To examine whether there exists any other influential factor related to source-emissions and processing effects on the BrC absorption we overlapped the AAE_{BrC} values⁷⁵ and the ratio of absorbance at 250 nm to 365 nm (A_{250}/A_{365}) in Figure 6. This is to understand the relative differences in the characteristics of constituent chromophores of BrC (*viz.*, strongly or weakly absorbing tendency, more or less aromatic, and high/low molecular weights) from the BoB and Visakhapatnam. The AAE_{MeOH-BrC} values over the BoB (5.5 ± 3.0) and Visakhapatnam (5.3 ± 1.3) during the southwest monsoon season are somewhat higher than the AAE_{H2O-BrC} (3.1 ± 1.1 and 3.5 ± 0.5 , respectively). Similar to our study, Cheng *et al.*⁶⁵ observed higher AAE_{BrC} for the methanol extracts than the water extracts of some aerosol samples collected over Beijing. Zhu *et al.*⁸² also noticed

higher AAE values for the methanol-soluble BrC (8.2 ± 1.4) than the water-soluble BrC (6.7 ± 0.8). Dasari *et al.*²⁶ have suggested that AAE_{BrC} increase from source-emissions in the IGP (Patiala: 5.3 ± 2.0 ²⁰; Delhi: 5.1 ± 2.0 ³⁰; Kharagpur: 6.0 ± 1.1 ²⁸) to the Indian Ocean (BoB: 9.1 ± 2.5 ²⁷ and Maldives: 7.2 ± 0.7 ²⁹) during the continental outflow due to ambient photochemical transformations (i.e., secondary BrC). Such high AAE_{BrC} values in the methanol extracts suggest that water-insoluble fraction of BrC over the BoB and Visakhapatnam is mostly secondary origin and the constituent chromophores are more absorptive at shorter wavelengths (< 365 nm). In contrast, the low AAE values for the water extract over the BoB and Visakhapatnam indicate that the BrC-chromophores are more absorptive at longer wavelengths (> 365 nm).

The A_{250}/A_{365} ratio can be used to understand the prevailing differences in the aromatic character and molecular weights of BrC chromophores⁸³⁻⁸⁵. Duarte *et al.*⁸⁶ have documented an inverse relationship between A_{250}/A_{365} and aromatic character/molecular weights of constituent chromophores in atmospheric aerosols. A_{250}/A_{365} ratio (aka E_2/E_3 in the literature) is somewhat lower for water extracts (2.3 -10.2; av. 4.4 ± 2.6) than methanol extracts (7.0 – 25.6; 11.8 ± 6.5) for PM_{10} samples collected over the BoB (Figure 6, see colour scale). A similar feature is observed for Visakhapatnam samples, where absorbance ratios of A_{250}/A_{365} for water-soluble BrC (2.3 – 4.8; av. 3.5 ± 0.8) were lower than methanol-soluble BrC (2.4 – 8.4; av. 5.4 ± 2.1). These results suggest that BrC chromophores in water-extracts of PM_{10} aerosols collected over the BoB and Visakhapatnam are enriched with aromatic structures with higher molecular weight compounds than methanol-soluble BrC chromophores.

3.5. Relative radiative forcing of BrC over EC

The fraction of solar radiation absorbed by water-soluble BrC compared to that of EC (aka RRF_{BrC}) over Visakhapatnam was estimated according to methods described in an earlier publications^{28, 30, 87, 88}. For assessing the RRF_{BrC} , we need the wavelength-dependent fraction of solar emission flux absorbed by the BrC (or the light-absorbing WSOC) and EC aerosols. This can be approximated by using their wavelength-dependent MAE_{λ} (i.e., $MAE_{\lambda_0} * (\lambda/\lambda_0)^{-AAE}$) and Lambert-Beer's law as given in Eqns 13 and 14.

$$\frac{I-I_0}{I}(\lambda, BrC_{H_2O/MeOH}) = 1 - e^{-\left(MAE_{BrC, \lambda_0} \times \left(\frac{\lambda}{\lambda_0}\right)^{-AAE_{BrC}} [WSOC \text{ or } OC] \times BLH\right)} \quad (13)$$

$$\frac{I-I_0}{I}(\lambda, EC) = 1 - e^{-\left(MAE_{EC, \lambda_0} \times \left(\frac{\lambda}{\lambda_0}\right)^{-AAE_{EC}} [EC] \times BLH\right)} \quad (14)$$

Here, we assumed the boundary layer height (BLH) as 2000 m as the aerosol samples from this study belong to the summer season. When MAE_{BrC-H_2O} and $MAE_{BrC-MeOH}$ were used in Eqn 13, accordingly we used WSOC and OC concentrations, respectively, for representing water-soluble and water-insoluble light-absorbing organic matter in aerosols. We further used the $MAE_{EC-660nm}$ and $MAE_{BrC-365nm}$ from each sample for this calculation. However, we chose a value of 1.0 for the AAE of EC in this study to have consistency for comparing the estimated RRF_{BrC} between this study and previous studies from the South Asian outflow. In above Eqns 13 and 14, the λ_0 corresponds to 365 nm for the light-absorbing WSOC and 660 nm for EC. Likewise, [WSOC] and [EC] refer to their mass concentrations and ‘ λ ’ is any wavelength between 300 nm and 2500 nm (*i.e.* range of available full scan spectrum of solar absorption data). Levinson *et al.*⁸⁹ have recently provided the solar emission flux ($I_0(\lambda)$) from the clear sky Air Mass 1 Global Horizontal (AM1GH), the solar irradiance model. By combining this solar emission flux ($I_0(\lambda)$) and the output from Eqns 13 and 14 to Eqn 15, we have estimated the fraction of solar radiation absorbed by the light-absorbing water-soluble BrC relative to that of EC in marine aerosols collected over the BoB and Visakhapatnam.

$$f = \frac{\int_{300}^{2500} I_0(\lambda) \times \frac{I-I_0}{I}(\lambda, BrC_{H_2O/MeOH})}{\int_{300}^{2500} I_0(\lambda) \times \frac{I-I_0}{I}(\lambda, EC)} \quad (15)$$

In a way, the numerator and denominator of Eqn 15 correspond to the fraction of solar radiation absorbed by BrC and EC, respectively (Figure 7). Because these ‘ f ’ values are the fraction of BrC absorbing sunlight relative to that of EC, it is commonly reported in their percentage of EC absorption. Our estimates of RRF_{BrC} over the BoB during September-October 2017 ($1.8 \pm 1.2\%$; $N = 5$) were significantly lower (two-tailed t-test; t-score = 5.5, df = 11; $p < 0.05$) than that sampled during November 2008 ($12 \pm 4\%$; $N = 8$)⁴⁰ as well as those sampled over Visakhapatnam. Likewise, no such significant differences ($t = 0.5$, df = 14, p -value > 0.05) were observed between water (av. $5 \pm 3\%$; $N = 8$) and methanol soluble BrC (av. $7 \pm 11\%$; $N = 8$) aerosols over Visakhapatnam. However, our RRF_{BrC} values over Visakhapatnam are comparable to those reported over the IGP ($\sim 40\%$ over Patiala²⁰; 3-11% over Delhi³⁰; $\sim 30\%$ over Kanpur³²; 2-34% over Kharagpur²⁸). Our study highlights the ubiquitous presence of water and methanol soluble BrC over Visakhapatnam as well as *BrC-like* aerosols over the BoB.

4. Summary and conclusions

We observe detectable levels of BrC absorption from the water and methanol extracts of PM_{10} samples collected over the BoB and Visakhapatnam (a coastal city in southern India) during the southwest monsoon, a transition period with a less continental influence than the winter season. The

absorption spectra of BrC between 200 nm and 700 nm over the BoB showed several peaks compared to a monotonous decrease observed over the Visakhapatnam. We found that the air mass BTs over the BoB mostly originate from the sea-side, indicating the marine source of BrC. The impact of marine-derived organic matter over the BoB is also evident by the high levels of WIOC/OC(%) and high enrichment factors of Mg^{2+} (*i.e.* biogenic origin from the sea) in aerosols collected during SSK105 cruise. Coincidentally, the surface water samples collected from the Gautami-Godavari estuary draining into the BoB showed the presence of CDOM, which has a characteristic near UV-visible absorption spectra similar to that of ambient BrC. This observation suggests a significant contribution of marine-derived BrC over the BoB during the southwest monsoon. In contrast, the absorption spectra and optical properties of BrC over Visakhapatnam are comparable to those reported for the biomass burning events in the IGP. Besides, the air mass BTs and firecount over Visakhapatnam revealed the impact of long-range transport of BrC from the biomass burning emissions in the IGP. Therefore, the fraction of *BrC-like* substances emitted from the ocean surface to ambient marine aerosols seems to be important for assessing the regional radiative forcing of light-absorbing organic compounds.

Acknowledgements

PB acknowledges the partial financial support from the DST-INSPIRE fellowship (DST/INSPIRE/04/2017/000324 dated 24/07/2017) and JASSO follow up research fellowship from Japan. PB is grateful to the Scientist-In-Charge and the Director of NIO for the support at the workplace. Authors are thankful to the Chief Scientist Dr. L. Jagadeesan and participants onboard of SSK105. PB is thankful for the comments provided by Dr Dileep Kumar and Dr. V.V.S.S.Sarma as well as the CDOM data obtained from the neritic waters of the Bay of Bengal by Prof. N.S. Sarma, Andhra University.

References

1. R. Saleh, E. S. Robinson, D. S. Tkacik, A. T. Ahern, S. Liu, A. C. Aiken, R. C. Sullivan, A. A. Presto, M. K. Dubey, R. J. Yokelson, N. M. Donahue and A. L. Robinson, Brownness of organics in aerosols from biomass burning linked to their black carbon content, *Nature Geoscience*, 2014, **7**, 647-650.
2. Y. Zhang, H. Forrister, J. Liu, J. Dibb, B. Anderson, J. P. Schwarz, A. E. Perring, J. L. Jimenez, P. Campuzano-Jost and Y. Wang, Top-of-atmosphere radiative forcing affected by brown carbon in the upper troposphere, *Nature Geoscience*, 2017, **10**, 486-489.
3. C. E. Chung, V. Ramanathan and D. Decremer, Observationally constrained estimates of carbonaceous aerosol radiative forcing, *Proceedings of the National Academy of Sciences*, 2012, **109**, 11624-11629.
4. Y. Feng, V. Ramanathan and V. Kotamarthi, Brown carbon: a significant atmospheric absorber of solar radiation?, *Atmospheric Chemistry and Physics*, 2013, **13**, 8607-8621.
5. T. C. Bond, S. J. Doherty, D. Fahey, P. Forster, T. Berntsen, B. DeAngelo, M. Flanner, S. Ghan, B. Kärcher and D. Koch, Bounding the role of black carbon in the climate system: A scientific assessment, *Journal of Geophysical Research: Atmospheres*, 2013, **118**, 5380-5552.
6. A. Laskin, J. Laskin and S. A. Nizkorodov, Chemistry of atmospheric brown carbon, *Chemical reviews*, 2015, **115**, 4335-4382.
7. M. O. Andreae and A. Gelencsér, Black carbon or brown carbon? The nature of light-absorbing carbonaceous aerosols, *Atmospheric Chemistry and Physics*, 2006, **6**, 3131-3148.
8. R. Bahadur, P. S. Praveen, Y. Xu and V. Ramanathan, Solar absorption by elemental and brown carbon determined from spectral observations, *Proceedings of the National Academy of Sciences*, 2012, doi: 10.1073/pnas.1205910109, 201205910.
9. R. K. Chakrabarty, H. Moosmüller, L. W. A. Chen, K. Lewis, W. P. Arnott, C. Mazzoleni, M. K. Dubey, C. E. Wold, W. M. Hao and S. M. Kreidenweis, Brown carbon in tar balls from smoldering biomass combustion, *Atmos. Chem. Phys.*, 2010, **10**, 6363-6370.
10. A. Hoffer, A. Gelencsér, P. Guyon, G. Kiss, O. Schmid, G. Frank, P. Artaxo and M. Andreae, Optical properties of humic-like substances (HULIS) in biomass-burning aerosols, *Atmospheric Chemistry and Physics*, 2006, **6**, 3563-3570.
11. X. Zhang, Y.-H. Lin, J. D. Surratt, P. Zotter, A. S. H. Prévôt and R. J. Weber, Light-absorbing soluble organic aerosol in Los Angeles and Atlanta: A contrast in secondary organic aerosol, *Geophysical Research Letters*, 2011, **38**, doi:10.1029/2011GL049385.
12. K. M. Updyke, T. B. Nguyen and S. A. Nizkorodov, Formation of brown carbon via reactions of ammonia with secondary organic aerosols from biogenic and anthropogenic precursors, *Atmospheric Environment*, 2012, **63**, 22-31.
13. H. Lukács, A. Gelencsér, S. Hammer, H. Puxbaum, C. Pio, M. Legrand, A. Kasper-Giebl, M. Handler, A. Limbeck, D. Simpson and S. Preunkert, Seasonal trends and possible sources of brown carbon based on 2-year aerosol measurements at six sites in Europe, *Journal of Geophysical Research: Atmospheres*, 2007, **112**, doi:10.1029/2006JD008151.

14. E. N. Kirillova, A. Marinoni, P. Bonasoni, E. Vuillermoz, M. C. Facchini, S. Fuzzi and S. Decesari, Light absorption properties of brown carbon in the high Himalayas, *Journal of Geophysical Research: Atmospheres*, 2016, **121**, 9621-9639.
15. D. A. Lack, J. M. Langridge, R. Bahreini, C. D. Cappa, A. M. Middlebrook and J. P. Schwarz, Brown carbon and internal mixing in biomass burning particles, *Proceedings of the National Academy of Sciences*, 2012, doi: 10.1073/pnas.1206575109.
16. G. Lin, J. E. Penner, M. G. Flanner, S. Sillman, L. Xu and C. Zhou, Radiative forcing of organic aerosol in the atmosphere and on snow: Effects of SOA and brown carbon, *Journal of Geophysical Research: Atmospheres*, 2014, **119**, 7453-7476.
17. P. Lin, P. K. Aiona, Y. Li, M. Shiraiwa, J. Laskin, S. A. Nizkorodov and A. Laskin, Molecular Characterization of Brown Carbon in Biomass Burning Aerosol Particles, *Environmental Science & Technology*, 2016, **50**, 11815-11824.
18. Y. Desyaterik, Y. Sun, X. Shen, T. Lee, X. Wang, T. Wang and J. L. Collett, Speciation of "brown" carbon in cloud water impacted by agricultural biomass burning in eastern China, *Journal of Geophysical Research: Atmospheres*, 2013, **118**, 7389-7399.
19. C. Mohr, F. D. Lopez-Hilfiker, P. Zotter, A. S. Prévôt, L. Xu, N. L. Ng, S. C. Herndon, L. R. Williams, J. P. Franklin and M. S. Zahniser, Contribution of nitrated phenols to wood burning brown carbon light absorption in Detling, United Kingdom during winter time, *Environmental Science & Technology*, 2013, **47**, 6316-6324.
20. S. Bikkina, N. Rastogi, M. Sarin, A. Singh and D. Singh, Mass absorption efficiency of light absorbing organic aerosols from source region of paddy-residue burning emissions in the Indo-Gangetic Plain, *Atmospheric Environment*, 2016, **125**, 360-370.
21. P. Shamjad, S. N. Tripathi, R. Pathak, M. Hallquist, A. Arola and M. H. Bergin, Contribution of Brown Carbon to Direct Radiative Forcing over the Indo-Gangetic Plain, *Environmental science & technology*, 2015, **49**, 10474-10481.
22. B. R. G. Mabato, M. Gen, Y. Chu and C. K. Chan, Reactive Uptake of Glyoxal by Methylammonium-Containing Salts as a Function of Relative Humidity, *ACS Earth and Space Chemistry*, 2019, **3**, 150-157.
23. C. Song, M. Gyawali, R. A. Zaveri, J. E. Shilling and W. P. Arnott, Light absorption by secondary organic aerosol from α -pinene: Effects of oxidants, seed aerosol acidity, and relative humidity, *Journal of Geophysical Research: Atmospheres*, 2013, **118**, 11,741-711,749.
24. H. J. Lee, P. K. Aiona, A. Laskin, J. Laskin and S. A. Nizkorodov, Effect of Solar Radiation on the Optical Properties and Molecular Composition of Laboratory Proxies of Atmospheric Brown Carbon, *Environmental Science & Technology*, 2014, **48**, 10217-10226.
25. S. Bikkina and M. Sarin, Brown Carbon in the continental outflow to the North Indian Ocean, *Environmental Science: Processes & Impacts*, 2019, doi: 10.1039/C9EM00089E.
26. S. Dasari, A. Andersson, S. Bikkina, H. Holmstrand, K. Budhavant, S. Satheesh, E. Asmi, J. Kesti, J. Backman, A. Salam, D. S. Bisht, S. Tiwari, Z. Hameed and Ö. Gustafsson,

Photochemical degradation affects the light absorption of water-soluble brown carbon in the South Asian outflow, *Science Advances*, 2019, **5**, eaau8066, doi: 8010.1126/sciadv.aau8066.

27. B. Srinivas and M. M. Sarin, Light absorbing organic aerosols (brown carbon) over the tropical Indian Ocean: impact of biomass burning emissions, *Environmental Research Letters*, 2013, **8**, 044042.
28. S. Bikkina and M. Sarin, Brown carbon in atmospheric outflow from the Indo-Gangetic Plain: Mass absorption efficiency and temporal variability, *Atmospheric Environment*, 2014, **89**, 835-843.
29. C. Bosch, A. Andersson, E. N. Kirillova, K. Budhavant, S. Tiwari, P. Praveen, L. M. Russell, N. D. Beres, V. Ramanathan and Ö. Gustafsson, Source - diagnostic dual - isotope composition and optical properties of water - soluble organic carbon and elemental carbon in the South Asian outflow intercepted over the Indian Ocean, *Journal of Geophysical Research: Atmospheres*, 2014, **119**, 11,743-711,759.
30. E. N. Kirillova, A. Andersson, S. Tiwari, A. K. Srivastava, D. S. Bisht and Ö. Gustafsson, Water - soluble organic carbon aerosols during a full New Delhi winter: Isotope - based source apportionment and optical properties, *Journal of Geophysical Research: Atmospheres*, 2014, **119**, 3476-3485.
31. R. Satish, P. M. Shamjad, N. M. Thamban, S. N. Tripathi and N. Rastogi, Temporal Characteristics of Brown Carbon over the Central Indo-Gangetic Plain, *Environmental Science & Technology*, 2017.
32. P. M. Shamjad, S. N. Tripathi, N. M. Thamban and H. Vreeland, Refractive Index and Absorption Attribution of Highly Absorbing Brown Carbon Aerosols from an Urban Indian City-Kanpur, *Scientific Reports*, 2016, **6**, 37735.
33. V. Choudhary, P. Rajput, D. K. Singh, A. K. Singh and T. Gupta, Light absorption characteristics of brown carbon during foggy and non-foggy episodes over the Indo-Gangetic Plain, *Atmospheric Pollution Research*, 2018, doi: 10.1016/j.apr.2017.11.012.
34. R. K. Chakrabarty, S. Pervez, J. C. Chow, J. G. Watson, S. Dewangan, J. Robles and G. Tian, Funeral Pyres in South Asia: Brown Carbon Aerosol Emissions and Climate Impacts, *Environmental Science & Technology Letters*, 2014, **1**, 44-48.
35. S. A. Guazzotti, D. T. Suess, K. R. Coffee, P. K. Quinn, T. S. Bates, A. Wisthaler, A. Hansel, W. P. Ball, R. R. Dickerson, C. Neusüß, P. J. Crutzen and K. A. Prather, Characterization of carbonaceous aerosols outflow from India and Arabia: Biomass/biofuel burning and fossil fuel combustion, *Journal of Geophysical Research: Atmospheres*, 2003, **108**, doi:10.1029/2002JD003277.
36. V. Ramanathan, P. J. Crutzen, J. Lelieveld, A. Mitra, D. Althausen, J. Anderson, M. Andreae, W. Cantrell, G. Cass and C. Chung, Indian Ocean Experiment: An integrated analysis of the climate forcing and effects of the great Indo - Asian haze, *Journal of Geophysical Research: Atmospheres*, 2001, **106**, 28371-28398.

37. N. V. H. K. Chari, N. S. Sarma, S. R. Pandi and K. N. Murthy, Seasonal and spatial constraints of fluorophores in the midwestern Bay of Bengal by PARAFAC analysis of excitation emission matrix spectra, *Estuarine, Coastal and Shelf Science*, 2012, **100**, 162-171.
38. S. R. Pandi, R. Kiran, N. S. Sarma, A. S. Srikanth, V. V. S. S. Sarma, M. S. Krishna, D. Bandyopadhyay, V. R. Prasad, T. Acharyya and K. G. Reddy, Contrasting phytoplankton community structure and associated light absorption characteristics of the western Bay of Bengal, *Ocean Dynamics*, 2014, **64**, 89-101.
39. M. Madhupratap, M. Gauns, N. Ramaiah, S. P. Kumar, P. Muraleedharan, S. De Sousa, S. Sardesai and U. Muraleedharan, Biogeochemistry of the Bay of Bengal: physical, chemical and primary productivity characteristics of the central and western Bay of Bengal during summer monsoon 2001, *Deep Sea Research Part II: Topical Studies in Oceanography*, 2003, **50**, 881-896.
40. S. Prasanna Kumar, P. Muraleedharan, T. Prasad, M. Gauns, N. Ramaiah, S. De Souza, S. Sardesai and M. Madhupratap, Why is the Bay of Bengal less productive during summer monsoon compared to the Arabian Sea?, *Geophysical Research Letters*, 2002, **29**, doi:10.1029/2002GL016013.
41. S. Prasanna Kumar, M. Nuncio, N. Ramaiah, S. Sardesai, J. Narvekar, V. Fernandes and J. T. Paul, Eddy-mediated biological productivity in the Bay of Bengal during fall and spring intermonsoons, *Deep Sea Research Part I: Oceanographic Research Papers*, 2007, **54**, 1619-1640.
42. S. Prasanna Kumar, M. Nuncio, J. Narvekar, A. Kumar, S. Sardesai, S. N. de Souza, M. Gauns, N. Ramaiah and M. Madhupratap, Are eddies nature's trigger to enhance biological productivity in the Bay of Bengal?, *Geophysical Research Letters*, 2004, **31**.
43. M. Sarin, A. Kumar, B. Srinivas, A. Sudheer and N. Rastogi, Anthropogenic sulphate aerosols and large Cl-deficit in marine atmospheric boundary layer of tropical Bay of Bengal, *Journal of atmospheric chemistry*, 2010, **66**, 1-10.
44. Y. Miyazaki, K. Kawamura, J. Jung, H. Furutani and M. Uematsu, Latitudinal distributions of organic nitrogen and organic carbon in marine aerosols over the western North Pacific, *Atmospheric Chemistry and Physics*, 2011, **11**, 3037-3049.
45. A. Hecobian, X. Zhang, M. Zheng, N. Frank, E. S. Edgerton and R. J. Weber, Water-Soluble Organic Aerosol material and the light-absorption characteristics of aqueous extracts measured over the Southeastern United States, *Atmos. Chem. Phys.*, 2010, **10**, 5965-5977.
46. Y. Chen and T. C. Bond, Light absorption by organic carbon from wood combustion, *Atmos. Chem. Phys.*, 2010, **10**, 1773-1787.
47. H. Moosmüller, R. K. Chakrabarty, K. M. Ehlers and W. P. Arnott, Absorption Ångström coefficient, brown carbon, and aerosols: basic concepts, bulk matter, and spherical particles, *Atmos. Chem. Phys.*, 2011, **11**, 1217-1225.
48. A. Andersson, A Model for the Spectral Dependence of Aerosol Sunlight Absorption, *ACS Earth and Space Chemistry*, 2017, **1**, 533-539.

49. H. Sun, L. Biedermann and T. C. Bond, Color of brown carbon: A model for ultraviolet and visible light absorption by organic carbon aerosol, *Geophysical Research Letters*, 2007, **34**, doi: 10.1029/2007GL029797.
50. J. Liu, M. Bergin, H. Guo, L. King, N. Kotra, E. Edgerton and R. Weber, Size-resolved measurements of brown carbon in water and methanol extracts and estimates of their contribution to ambient fine-particle light absorption, *Atmospheric Chemistry and Physics*, 2013, **13**, 12389-12404.
51. K. J. Zarzana, C. D. Cappa and M. A. Tolbert, Sensitivity of Aerosol Refractive Index Retrievals Using Optical Spectroscopy, *Aerosol Science and Technology*, 2014, **48**, 1133-1144.
52. H. Moosmüller, R. K. Chakrabarty and W. P. Arnott, Aerosol light absorption and its measurement: A review, *Journal of Quantitative Spectroscopy and Radiative Transfer*, 2009, **110**, 844-878.
53. B. J. Sumlin, C. R. Oxford, B. Seo, R. R. Pattison, B. J. Williams and R. K. Chakrabarty, Density and Homogeneous Internal Composition of Primary Brown Carbon Aerosol, *Environmental Science & Technology*, 2018, **52**, 3982-3989.
54. J. Rissler, E. Z. Nordin, A. C. Eriksson, P. T. Nilsson, M. Frosch, M. K. Sporre, A. Wierzbicka, B. Svenningsson, J. Löndahl, M. E. Messing, S. Sjogren, J. G. Hemmingsen, S. Loft, J. H. Pagels and E. Swietlicki, Effective Density and Mixing State of Aerosol Particles in a Near-Traffic Urban Environment, *Environmental Science & Technology*, 2014, **48**, 6300-6308.
55. J. Mok, N. A. Krotkov, A. Arola, O. Torres, H. Jethva, M. Andrade, G. Labow, T. F. Eck, Z. Li, R. R. Dickerson, G. L. Stenchikov, S. Osipov and X. Ren, Impacts of brown carbon from biomass burning on surface UV and ozone photochemistry in the Amazon Basin, *Scientific Reports*, 2016, **6**, 36940.
56. J. S. Reid, R. Koppmann, T. F. Eck and D. P. Eleuterio, A review of biomass burning emissions part II: intensive physical properties of biomass burning particles, *Atmos. Chem. Phys.*, 2005, **5**, 799-825.
57. Y. Miyazaki, S. G. Aggarwal, K. Singh, P. K. Gupta and K. Kawamura, Dicarboxylic acids and water-soluble organic carbon in aerosols in New Delhi, India, in winter: Characteristics and formation processes, *Journal of Geophysical Research: Atmospheres*, 2009, **114**.
58. K. Ram and M. Sarin, Absorption coefficient and site-specific mass absorption efficiency of elemental carbon in aerosols over urban, rural, and high-altitude sites in India, *Environmental science & technology*, 2009, **43**, 8233-8239.
59. E. Weingartner, H. Saathoff, M. Schnaiter, N. Streit, B. Bitnar and U. Baltensperger, Absorption of light by soot particles: determination of the absorption coefficient by means of aethalometers, *Journal of Aerosol Science*, 2003, **34**, 1445-1463.
60. A. Stein, R. Draxler, G. Rolph, B. Stunder, M. Cohen and F. Ngan, NOAA's HYSPLIT atmospheric transport and dispersion modeling system, *Bulletin of the American Meteorological Society*, 2015, **96**, 2059-2077.

61. R. Satish and N. Rastogi, On the Use of Brown Carbon Spectra as a Tool to Understand Their Broader Composition and Characteristics: A Case Study from Crop-residue Burning Samples, *ACS Omega*, 2019, **4**, 1847-1853.
62. A. Rana, S. Dey, P. Rawat, A. Mukherjee, J. Mao, S. Jia, P. S. Khillare, A. K. Yadav and S. Sarkar, Optical properties of aerosol brown carbon (BrC) in the eastern Indo-Gangetic Plain, *Science of The Total Environment*, 2020, **716**, 137102.
63. C.-S. Zhu, J.-J. Cao, T.-F. Hu, Z.-X. Shen, X.-X. Tie, H. Huang, Q.-Y. Wang, R.-J. Huang, Z.-Z. Zhao, G. Močnik and A. D. A. Hansen, Spectral dependence of aerosol light absorption at an urban and a remote site over the Tibetan Plateau, *Science of The Total Environment*, 2017, **590-591**, 14-21.
64. C. Yan, M. Zheng, A. P. Sullivan, C. Bosch, Y. Desyaterik, A. Andersson, X. Li, X. Guo, T. Zhou, Ö. Gustafsson and J. L. Collett, Chemical characteristics and light-absorbing property of water-soluble organic carbon in Beijing: Biomass burning contributions, *Atmospheric Environment*, 2015, **121**, 4-12.
65. Y. Cheng, K.-b. He, Z.-y. Du, G. Engling, J.-m. Liu, Y.-l. Ma, M. Zheng and R. J. Weber, The characteristics of brown carbon aerosol during winter in Beijing, *Atmospheric Environment*, 2016, **127**, 355-364.
66. C. Yan, M. Zheng, C. Bosch, A. Andersson, Y. Desyaterik, A. P. Sullivan, J. L. Collett, B. Zhao, S. Wang, K. He and Ö. Gustafsson, Important fossil source contribution to brown carbon in Beijing during winter, *Scientific Reports*, 2017, **7**, 43182.
67. Y. Lei, Z. Shen, Q. Wang, T. Zhang, J. Cao, J. Sun, Q. Zhang, L. Wang, H. Xu, J. Tian and J. Wu, Optical characteristics and source apportionment of brown carbon in winter PM_{2.5} over Yulin in Northern China, *Atmospheric Research*, 2018, **213**, 27-33.
68. S. Bikkina, M. M. Haque, M. Sarin and K. Kawamura, Tracing the relative significance of primary versus secondary organic aerosols from biomass burning plumes over Coastal Ocean using sugar compounds and stable carbon isotopes, *ACS Earth and Space Chemistry*, 2019, **3**, 1471-1484.
69. N. S. Sarma, S. R. Pandi, N. Chari, G. Chiranjeevulu, R. Kiran, K. S. Krishna, D. B. Rao, P. Venkatesh, B. C. Kumar and A. Raman, Spectral modelling of estuarine coloured dissolved organic matter, *CURRENT SCIENCE*, 2018, **114**, 1762.
70. C. D. O'Dowd, M. C. Facchini, F. Cavalli, D. Ceburnis, M. Mircea, S. Decesari, S. Fuzzi, Y. J. Yoon and J.-P. Putaud, Biogenically driven organic contribution to marine aerosol, *Nature*, 2004, **431**, 676.
71. C. M. Sultana, D. B. Collins and K. A. Prather, Effect of Structural Heterogeneity in Chemical Composition on Online Single-Particle Mass Spectrometry Analysis of Sea Spray Aerosol Particles, *Environmental Science & Technology*, 2017, **51**, 3660-3668.
72. P. Bikkina, K. Kawamura, S. Bikkina, B. Kunwar, K. Tanaka and K. Suzuki, Hydroxy Fatty Acids in Remote Marine Aerosols over the Pacific Ocean: Impact of Biological Activity and Wind Speed, *ACS Earth and Space Chemistry*, 2019, **3**, 366-379.

73. T. Jayarathne, C. M. Sultana, C. Lee, F. Malfatti, J. L. Cox, M. A. Pendergraft, K. A. Moore, F. Azam, A. V. Tivanski and C. D. Cappa, Enrichment of saccharides and divalent cations in sea spray aerosol during two phytoplankton blooms, *Environmental Science & Technology*, 2016, **50**, 11511-11520.
74. P. M. Shamjad, R. V. Satish, N. M. Thamban, N. Rastogi and S. N. Tripathi, Absorbing Refractive Index and Direct Radiative Forcing of Atmospheric Brown Carbon over Gangetic Plain, *ACS Earth and Space Chemistry*, 2017, doi: 10.1021/acsearthspacechem.7b00074.
75. X. Li, Y. Yang, S. Liu, Q. Zhao, G. Wang and Y. Wang, Light absorption properties of brown carbon (BrC) in autumn and winter in Beijing: Composition, formation and contribution of nitrated aromatic compounds, *Atmospheric Environment*, 2020, **223**, 117289.
76. J. Liu, E. Scheuer, J. Dibb, G. S. Diskin, L. D. Ziemba, K. L. Thornhill, B. E. Anderson, A. Wisthaler, T. Mikoviny, J. J. Devi, M. Bergin, A. E. Perring, M. Z. Markovic, J. P. Schwarz, P. Campuzano-Jost, D. A. Day, J. L. Jimenez and R. J. Weber, Brown carbon aerosol in the North American continental troposphere: sources, abundance, and radiative forcing, *Atmos. Chem. Phys.*, 2015, **15**, 7841-7858.
77. J. Yan, X. Wang, P. Gong, C. Wang and Z. Cong, Review of brown carbon aerosols: Recent progress and perspectives, *Science of The Total Environment*, 2018, **634**, 1475-1485.
78. X. Zhang, Y.-H. Lin, J. D. Surratt and R. J. Weber, Sources, Composition and Absorption Ångström Exponent of Light-absorbing Organic Components in Aerosol Extracts from the Los Angeles Basin, *Environmental Science & Technology*, 2013, **47**, 3685-3693.
79. Y. Mo, J. Li, J. Liu, G. Zhong, Z. Cheng, C. Tian, Y. Chen and G. Zhang, The influence of solvent and pH on determination of the light absorption properties of water-soluble brown carbon, *Atmospheric Environment*, 2017, **161**, 90-98.
80. B. J. Turpin and H.-J. Lim, Species contributions to PM_{2.5} mass concentrations: Revisiting common assumptions for estimating organic mass, *Aerosol Science & Technology*, 2001, **35**, 602-610.
81. S. Bikkina and M. M. Sarin, PM_{2.5}, EC and OC in atmospheric outflow from the Indo-Gangetic Plain: Temporal variability and aerosol organic carbon-to-organic mass conversion factor, *The Science of the total environment*, 2014, **487**, 196.
82. C.-S. Zhu, J.-J. Cao, R.-J. Huang, Z.-X. Shen, Q.-Y. Wang and N.-N. Zhang, Light absorption properties of brown carbon over the southeastern Tibetan Plateau, *Science of The Total Environment*, 2018, **625**, 246-251.
83. Q. Chen, Z. Mu, W. Song, Y. Wang, Z. Yang, L. Zhang and Y.-L. Zhang, Size-Resolved Characterization of the Chromophores in Atmospheric Particulate Matter From a Typical Coal-Burning City in China, *Journal of Geophysical Research: Atmospheres*, 2019, **124**, 10546-10563.
84. S. Yue, S. Bikkina, M. Gao, L. A. Barrie, K. Kawamura and P. Fu, Sources and Radiative Absorption of Water-Soluble Brown Carbon in the High Arctic Atmosphere, *Geophysical Research Letters*, 2019, **46**, 14881-14891.

85. S. Tserenpil, X. J. Fan, A. Sapkota, E. Chinzorig, J. Z. Song and C. Q. Liu, High molecular weight humic-like substances in carboneous aerosol of Ulaanbaatar city, *Mongolian Journal of Chemistry*, 2018, **19**, 5-11.
86. R. M. B. O. Duarte, C. A. Pio and A. C. Duarte, Spectroscopic study of the water-soluble organic matter isolated from atmospheric aerosols collected under different atmospheric conditions, *Analytica Chimica Acta*, 2005, **530**, 7-14.
87. S. Bikkina and M. Sarin, Brown carbon in the continental outflow to the North Indian Ocean, *Environmental Science: Processes & Impacts*, 2019, **21**, 970-987.
88. E. N. Kirillova, A. Andersson, J. Han, M. Lee and Ö. Gustafsson, Sources and light absorption of water-soluble organic carbon aerosols in the outflow from northern China, *Atmospheric Chemistry and Physics*, 2014, **14**, 1413-1422.
89. R. Levinson, H. Akbari and P. Berdahl, Measuring solar reflectance—Part I: Defining a metric that accurately predicts solar heat gain, *Solar Energy*, 2010, **84**, 1717-1744.
90. W. C. Keene, A. A. Pszenny, J. N. Galloway and M. E. Hawley, Sea - salt corrections and interpretation of constituent ratios in marine precipitation, *Journal of Geophysical Research: Atmospheres (1984 -2012)*, 1986, **91**, 6647-6658.
91. S. Bikkina and M. M. Sarin, Light absorbing organic aerosols (brown carbon) over the tropical Indian Ocean: impact of biomass burning emissions, *Environmental research letters*, 2013, **8**, 044042.
92. K. Kawamura and S. Bikkina, A review of dicarboxylic acids and related compounds in atmospheric aerosols: Molecular distributions, sources and transformation, *Atmospheric Research*, 2016, **170**, 140-160.
93. H. Kim, J. Y. Kim, H. C. Jin, J. Y. Lee and S. P. Lee, Seasonal variations in the light-absorbing properties of water-soluble and insoluble organic aerosols in Seoul, Korea, *Atmospheric Environment*, 2016, **129**, 234-242.
94. C. Sarkar, C. Venkataraman, S. Yadav, H. C. Phuleria and A. Chatterjee, Origin and properties of soluble brown carbon in freshly emitted and aged ambient aerosols over an urban site in India, *Environmental Pollution*, 2019, **254**, 113077.

Table 1. Statistical summary of mass concentrations, diagnostic mass ratios, and absorption properties of BrC and EC aerosols collected over the Bay of Bengal and Visakhapatnam.

Species	Bay of Bengal	Visakhapatnam
	Min-Max (Av±Sd)	Min-Max (Av±Sd)
Na ⁺	3.9 - 7.2 (5.5±1.3)	2.8 - 10.3 (6.4±2.4)
K ⁺	0.8 - 1.1 (0.9±0.2)	0.6 - 2.4 (1.1±0.6)
NO ₃ ⁻	5.7 - 8.6 (7.0±1.0)	2.2 - 11.3 (4.8±2.7)
SO ₄ ²⁻	15.2 - 52.0 (26.7±13.4)	11.1 - 64.8 (25.6±17.0)
OC	4.6 - 7.8 (6.9±1.1)	2.6 - 9.8 (5.0±2.2)
EC	1.1 - 1.9 (1.5±0.3)	1.4 - 4.1 (2.3±0.9)
WSOC	0.64 - 0.94 (0.76±0.11)	0.89 - 2.20 (1.31±0.41)
WIOC	3.9 - 7.0 (6.2±1.0)	1.6 - 7.6 (3.7±1.8)
WSOC/OC	0.09 - 0.14 (0.11±0.02)	0.19 - 0.39(0.28±0.07)
WIOC/OC	0.86- 0.91 (0.89±0.02)	0.61 - 0.81 (0.72±0.07)
nss-K ⁺	0.52 - 0.83 (0.69±0.10)	0.42 - 2.1 (0.84±0.54)
nss-SO ₄ ²⁻	14.0 - 50.3 (25.3±13.2)	10.4 - 62.2 (24.0±16.5)
$b_{\text{abs-H}_2\text{O-BrC-365 nm}}$ (Mm ⁻¹)	0.12-0.96 (0.45±0.25)	1.30 - 4.30 (2.21±0.89)
MAE _{H₂O-BrC-365 nm} (m ² g ⁻¹)	0.16-1.45 (0.61±0.38)	1.08 - 3.18 (1.77±0.78)
AAE _{H₂O-BrC}	1.85-4.8 (3.1±1.1)	3.0 - 4.3 (3.5±0.5)
$b_{\text{abs-MeOH-BrC-365}}$ (Mm ⁻¹)	0.11-0.44 (0.27±0.11)	0.98 -7.38 (3.19±2.52)
MAE _{MeOH-BrC-365} (m ² g ⁻¹)	0.01-0.07 (0.04±0.02)	0.17 - 2.83 (0.89±1.07)
AAE _{MeOH-BrC}	3.0-10.0 (5.5±3.0)	3.4 - 7.1 (5.3±1.3)

Here $M = 10^6$, non-sea-salt or $\text{nss-K}^+ = \text{K}^+ - 0.037 \times \text{Na}^+$, $\text{nss-SO}_4^{2-} = \text{SO}_4^{2-} - 0.253 \times \text{Na}^+$ and $\text{WIOC} = \text{OC} - \text{WSOC}$. The non-sea-salt fractions were estimated by subtracting the sea salt component values and the factors 0.037 and 0.253 are the weight ratios of K^+/Na^+ and $\text{SO}_4^{2-}/\text{Na}^+$ in seawater⁹⁰.

Table 2. Comparison of absorption properties of water-soluble BrC aerosols from the Bay of Bengal (SSK105) and Visakhapatnam with other studies from S. Asia

Site	$b_{\text{abs-H}_2\text{O-BrC-365 nm}}$ (Mm^{-1})	$b_{\text{abs-MeOH-BrC-365 nm}}$ (Mm^{-1})	$\text{MAE}_{\text{H}_2\text{O-BrC-365nm}}$ ($\text{m}^2 \text{g}^{-1}$)	$\text{MAE}_{\text{MeOH-BrC-365nm}}$ ($\text{m}^2 \text{g}^{-1}$)	$\text{AAE}_{\text{H}_2\text{O-BrC}}$	$\text{AAE}_{\text{MeOH-BrC}}$	Reference
Bay of Bengal (SSK105)	0.12 -0.96 (0.45±0.25)	0.11-0.44 (0.27±0.11)	0.16 – 1.45 (0.61±0.38)	0.01-0.07 (0.04±0.02)	1.9 -4.8 (3.1±1.1)	3.0-10.0 (5.5±3.0)	This study
Visakhapatnam	1.6 -4.3 (2.3±0.9)	0.98 -7.38 (3.19±2.52)	0.48 -2.65 (1.16±0.78)	0.17 - 2.83 (0.89±1.07)	3.0 - 4.3 (3.5±0.5)	3.4 - 7.1 (5.3±1.3)	This study
Bay of Bengal (SS259)	1.2 -8.1 (4.2±1.8)	-	0.43 -0.67 (0.57±0.08)	-	4.5-6.5 (5.7±0.8)	-	Bikkina and Sarin ⁹¹
Arabian Sea (SS259)	0.4 -8.0 (3.2±2.1)	-	0.30 -1.52 (0.59±0.29)	-	1.1 -8.4 (5.9±1.8)	-	Bikkina and Sarin ⁹¹
Bay of Bengal (SK254)	0.2 - 3.9 (1.5±1.1)	-	0.22 - 0.75 (0.45±0.14)	-	2.5-19.1 (9.1±3.6)	-	Bikkina and Sarin ⁹¹
Patiala, India	19 -106 (52±27)	-	0.7 -2.5 (1.3±0.5)	-	2.3 - 10.9 (5.3±2.0)	-	Kawamura and Bikkina ⁹²
Delhi, India	-	-	2.2 -2.9 (2.5±0.2)	-	4.6 - 5.0 (4.8±0.2)	-	
Kharagpur, India	1.8 - 21.4 (11.4 ± 4.8)	-	0.21 - 1.46 (0.78±0.25)	-	2.5 - 15.5 (8.4±2.6)	-	Bikkina and Sarin ²⁸
Bhola, Bangladesh	-	-	0.8 - 1.7 (1.4±0.2)	-	5.7 - 6.7 (6.1±0.3)	-	Dasari <i>et al.</i> ²⁶
MCOH, Maldives	-	-	0.3 - 0.6 (0.4±0.1)	-	6.1 - 7.6 (6.9±0.4)	-	Dasari <i>et al.</i> ²⁶
Xi'an, northwest China	1.0 - 6.2 (3.1±2.5)	2.0 - 20.7 (9.6±8.8)	-	-	6.4 - 10.2 (7.9±1.6)	3.8 - 9.2 (6.3±1.9)	Shen <i>et al.</i> , 2017
Beijing	10.2 ± 6.9	26.2 ± 18.8	1.2 ± 0.11	1.4 ± 0.3	7.3 ± 0.2	7.1 ± 0.4	Cheng <i>et al.</i> , AE, 2016
NCOP, Nepal	1.83 ± 1.46	2.86 ± 2.49	0.72 ± 0.15	0.77 ± 0.18	5.1 ± 0.3	3.9 ± 0.6	Kirillova <i>et al.</i> ¹⁴
Seoul, Korea	3.39 ± 2.45	6.81 ± 2.59	0.28–1.18	0.44–1.45	7.23 ± 1.58	5.05 ± 0.67	Kim <i>et al.</i> ⁹³
Kanpur, India	69.3 ± 24.5	-	1.8 ± 0.2	-	2.8 ± 0.6		Choudhary <i>et al.</i> ³³
Yulin, Northern China	8.9±4.9	27.5 ± 12.0		1.4 ± 0.4	5.2± 0.8	4.9± 1.2	Lei <i>et al.</i> ⁶⁷
Mumbai, India	16.5 ± 7.3	33.3 ± 14.3	1.4 ± 0.4	2.3 ± 0.7	41.-8.9	5-6.5	Sarkar <i>et al.</i> ⁹⁴
West Bengal, India	9.7 ± 7.8	17.2 ± 9.0	0.95 ± 0.45	1.17 ± 0.78	5.91 ± 0.52	5.89 ± 0.21	Rana <i>et al.</i> ⁶²

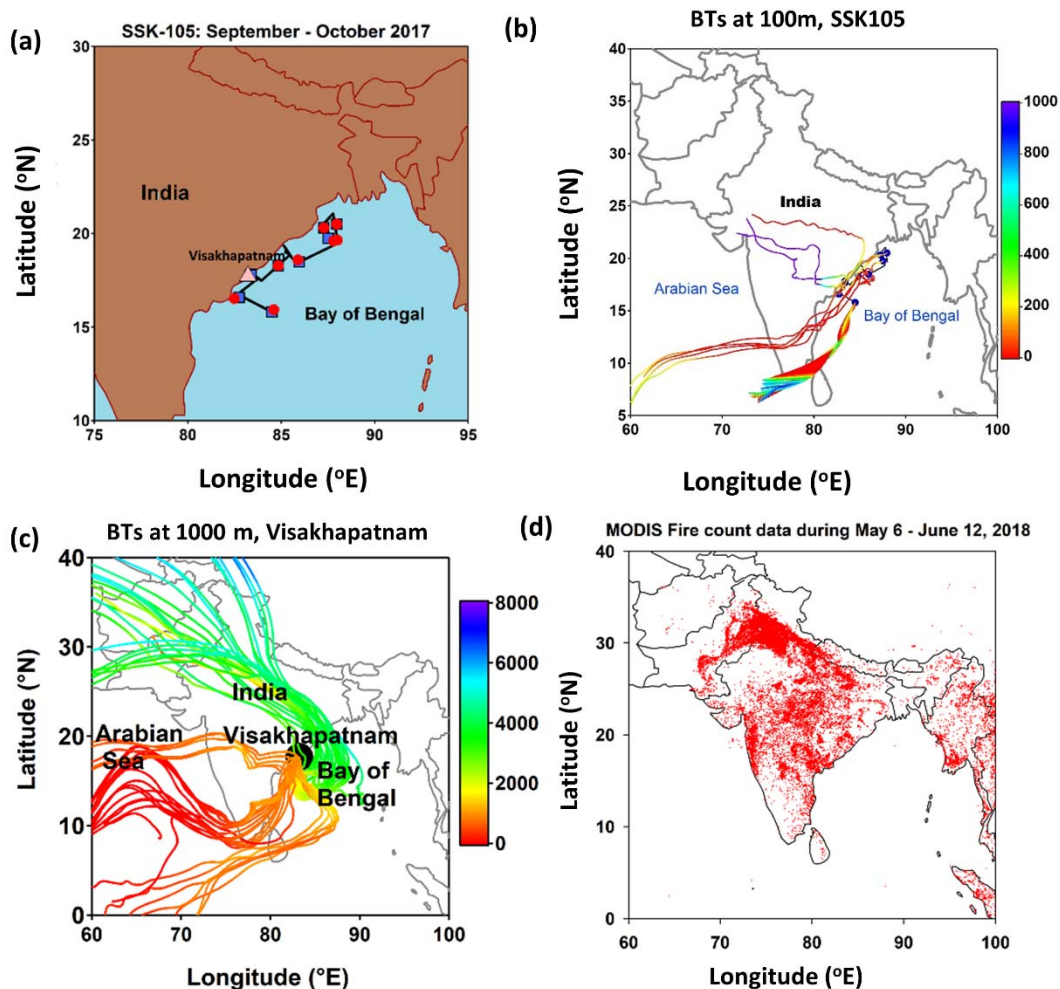


Figure 1. (a) Cruise track of SSK105 in the BoB (22 September – 4 October 2017; see blue line), 7-day air mass backward trajectories (BTs) computed at an arrival height of (b) 100 m over the BoB, and (c) 1000 m over Visakhapatnam (16 May-4June, 2018), (d) MODIS fire count data over South Asia (6 May - 12 June 2018). Here, the colour scale indicates the height of air mass back trajectories expressed in meters. The red dots in panel (a) correspond to the midpoint latitude and longitude of cruise tracks used for PM_{10} collection in the BoB.

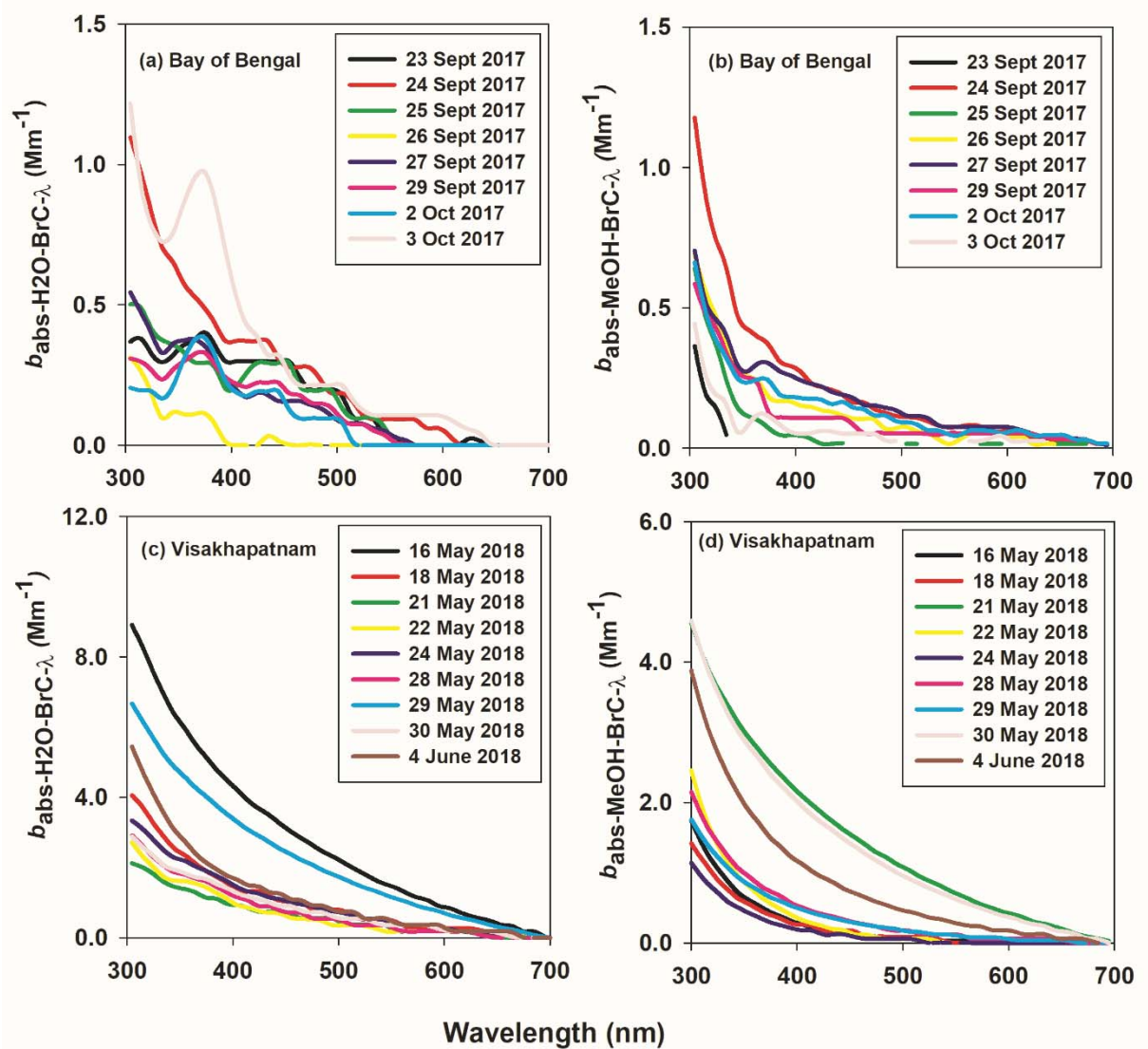


Figure 2. Wavelength dependence of absorption coefficient of water-soluble BrC (a,c) and methanol-soluble BrC (b,d) in aerosols (expressed in Mm^{-1} ; $M = 10^6$) collected over the Bay of Bengal and Visakhapatnam, respectively.

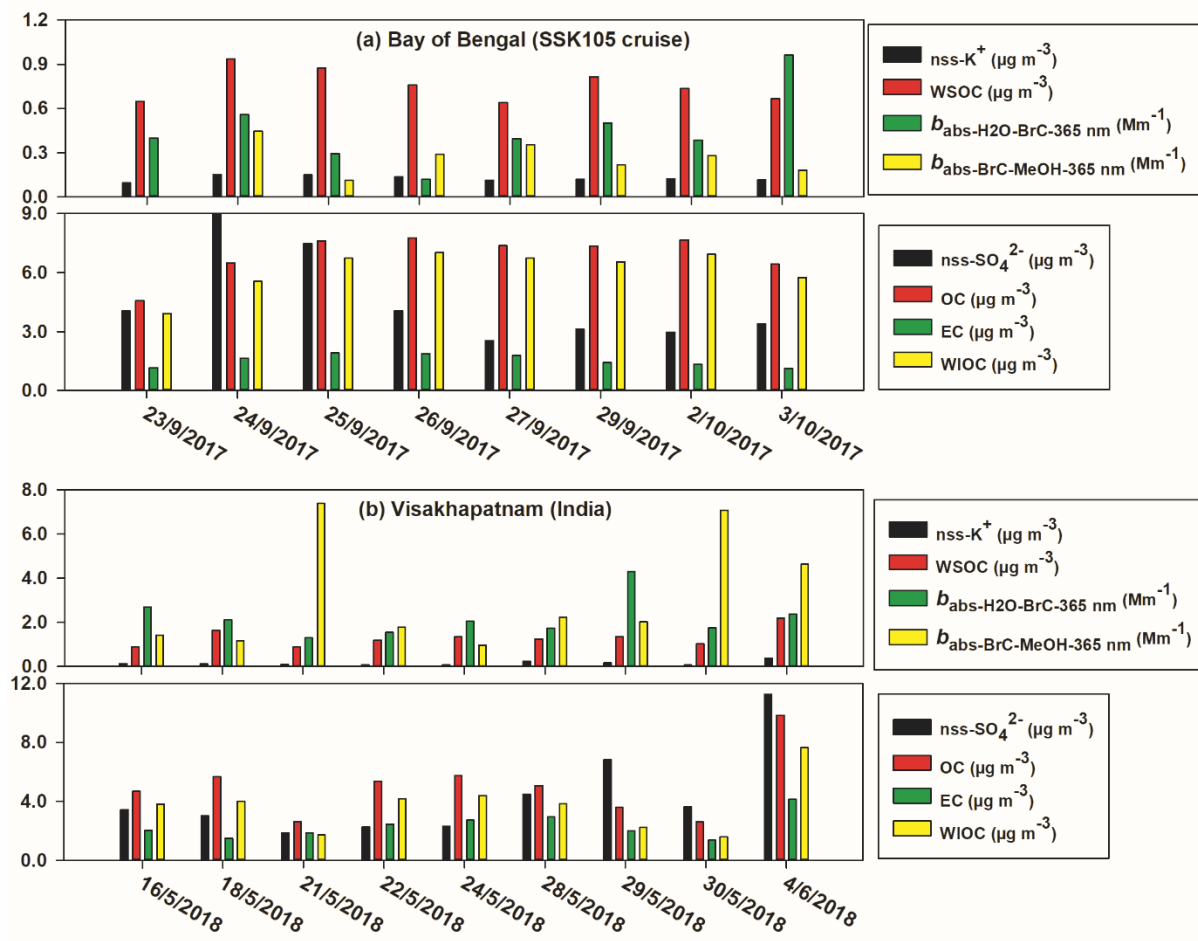


Figure 3. Bar graphs of mass concentrations of non-sea-salt or $nss-K^+$, WSOC, $nss-SO_4^{2-}$, OC, EC and WIOC along with absorption coefficient of BrC from the water and methanol extracts of PM_{10} samples collected over (a) the Bay of Bengal and (b) Visakhapatnam.

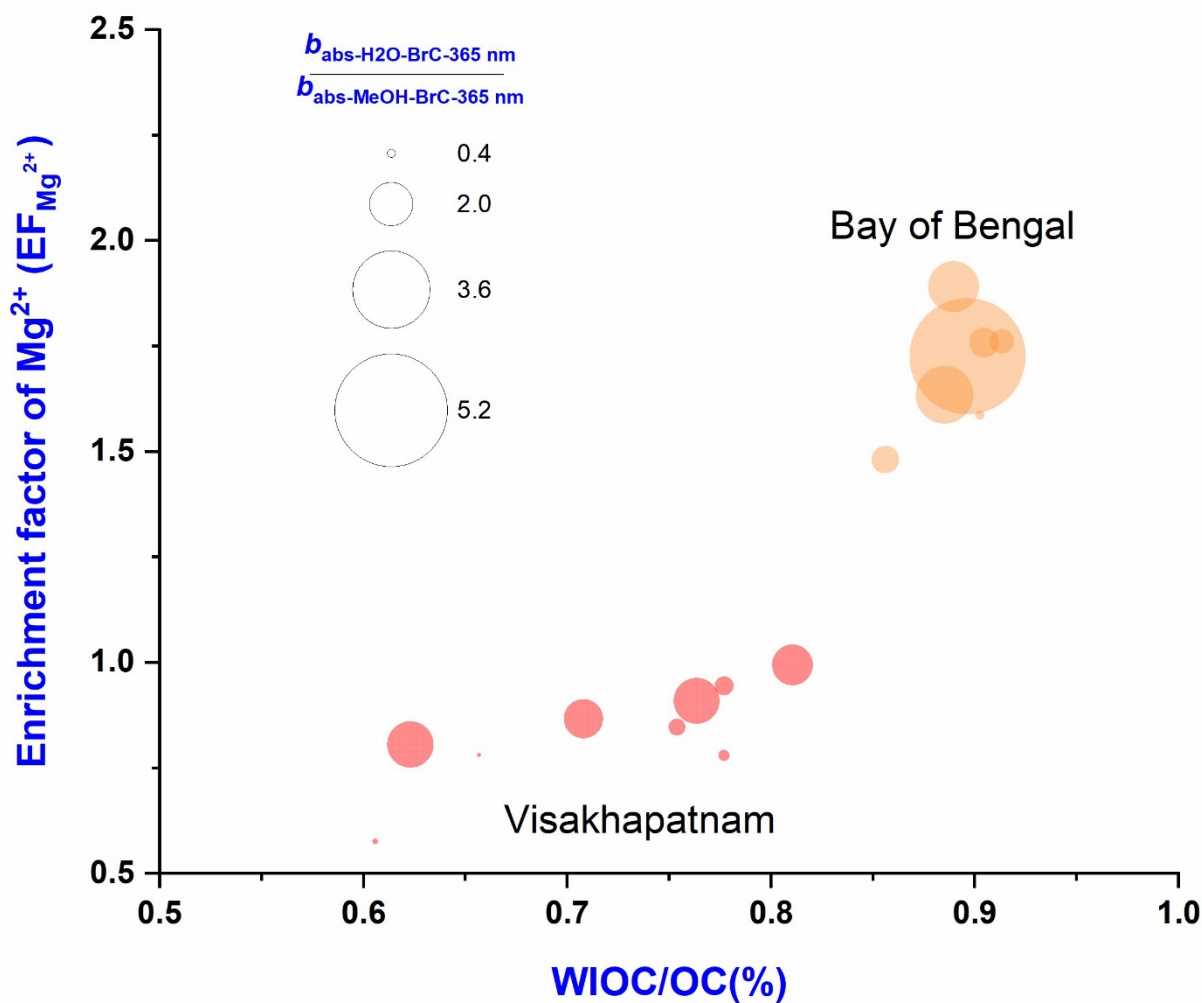


Figure 4. Scatter plot between percentage contribution of water-insoluble organic carbon (WIOC \approx OC-WSOC) in OC and enrichment factor of Mg^{2+} ($EF_{Mg^{2+}} = (Mg^{2+}/Na^+)_{aerosol} / (Mg^{2+}/Na^+)_{seawater}$) as a function of the ratio of the absorption coefficient of water-soluble BrC to that of methanol-soluble BrC in PM_{10} collected over the Bay of Bengal during SSK 105 cruise (23 September – 3 October 2017) and Visakhapatnam (16 May – 4 June 2018).

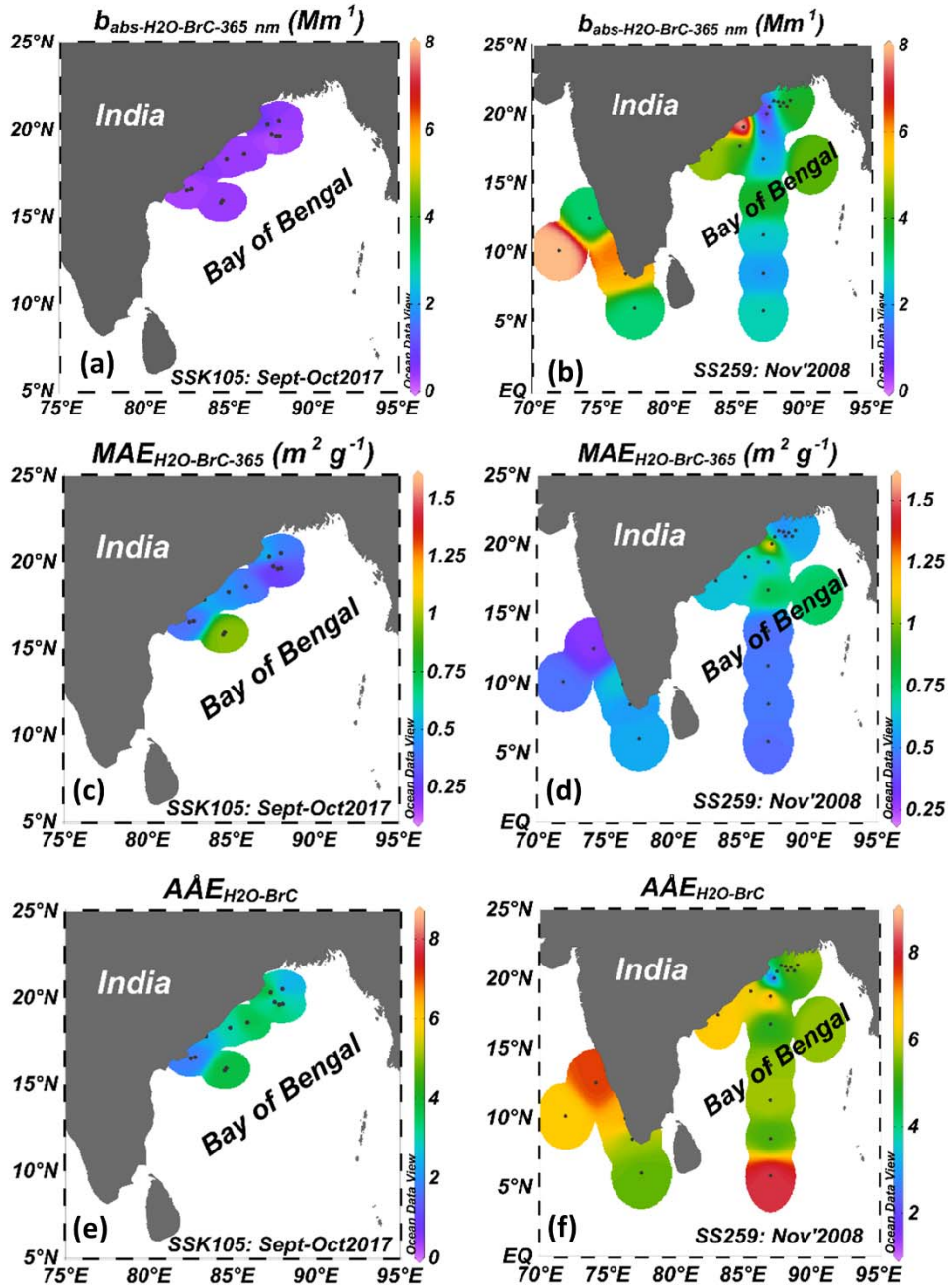


Figure 5. (a) Spatial variability of water-soluble BrC absorption coefficient ($b_{\text{abs-H2O-BrC-365}}$; $M = 10^{-6}$), (b) mass absorption efficiency ($MAE_{H2O-BrC-365}$) and (c) absorption angstrom exponent (AAE_{BrC}) in aerosols collected over the Bay of Bengal between southwest monsoon (SSK105; left panels) and northeast monsoon (SS259: November 2008²⁷; right panels).

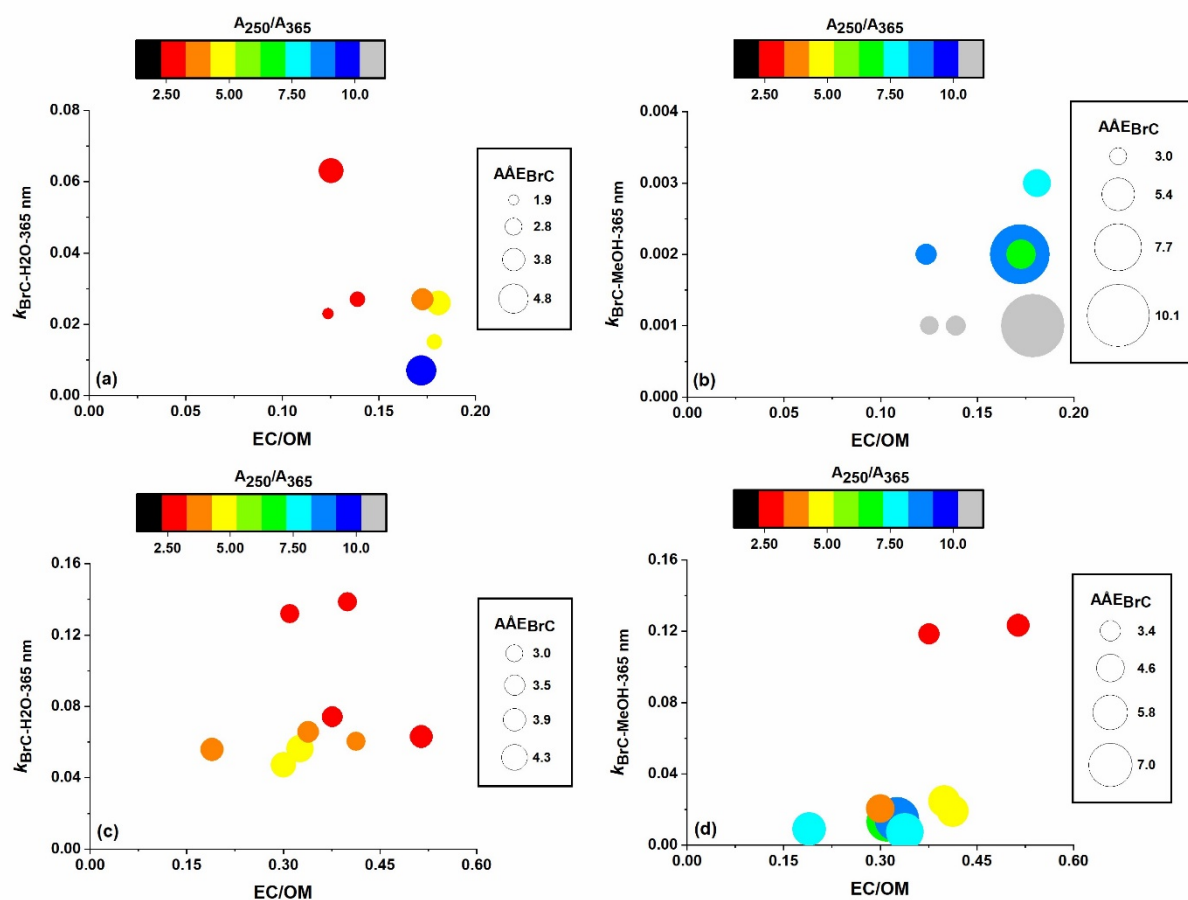


Figure 6. Scatter plot of the refractive index of BrC from water and methanol extracts and methanol extracts versus the mass ratio of EC/OM (i.e., $OC \times 1.4$) in PM_{10} samples collected over the BoB and Visakhapatnam, respectively, as a function of absorption ångström exponent (AAE_{BrC}) and the ratio of absorbance at 250 nm to that at 365 nm.

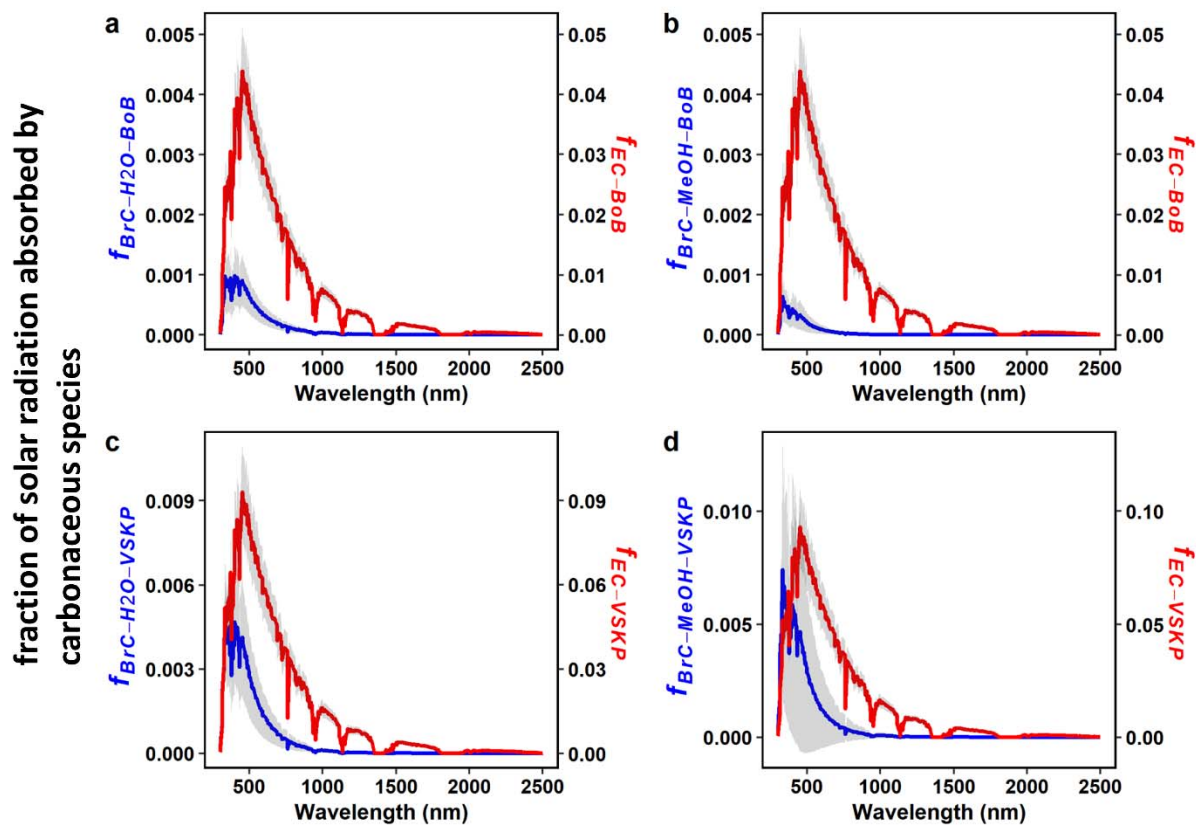
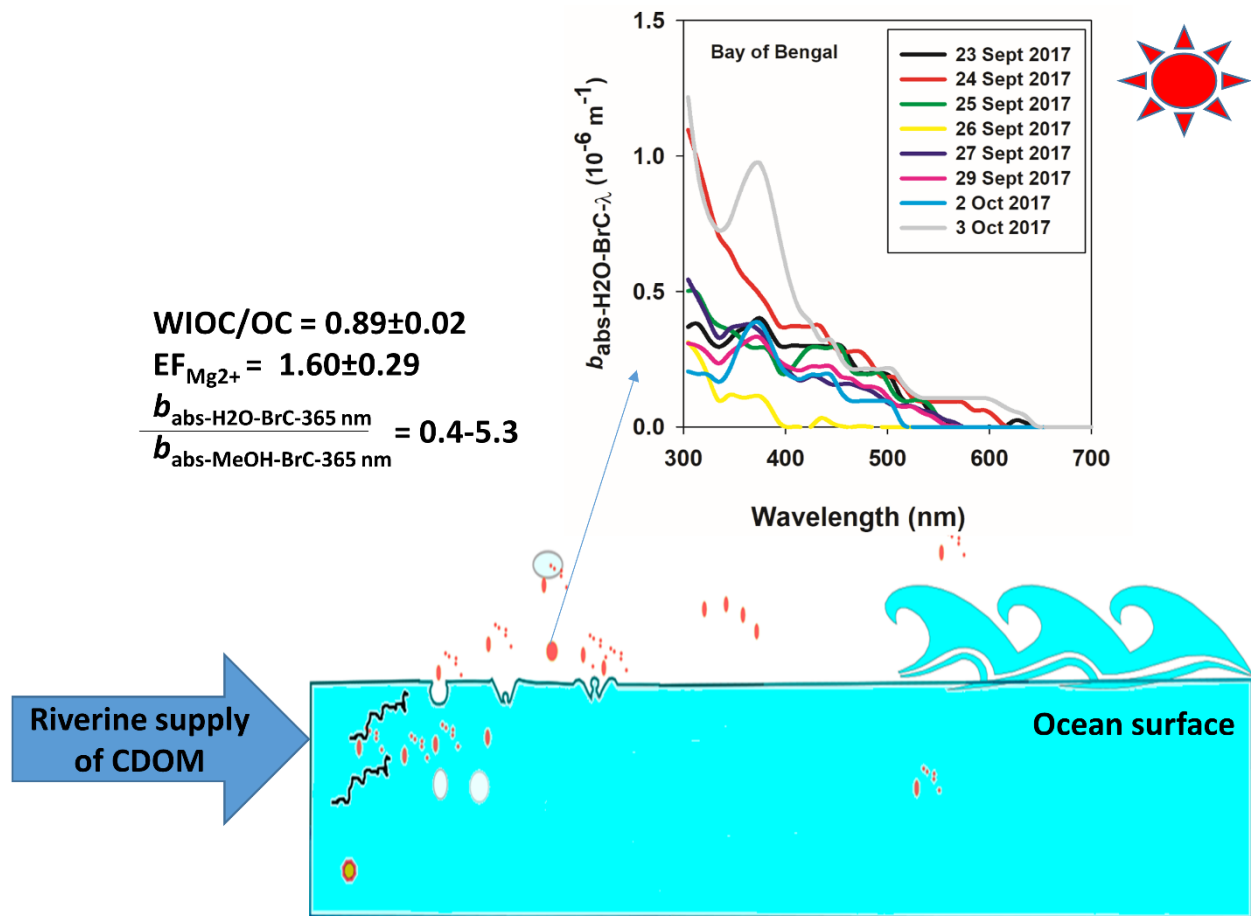


Figure 7. Fraction of solar radiation (blue colour) absorbed by the BrC from the water-soluble (left panel) and methanol (right panel) soluble extracts of aerosols sampled over the (a, b) BoB and (c, d) Visakhapatnam along with the fraction sunlight (red colour) absorbed by the EC (right axis) for the respective samples.



Graphic Abstract

Supplementary information for

Evidence for the brown carbon absorption over the Bay of Bengal during the southwest monsoon season: a possible oceanic source

By Poonam Bikkina et al.

“Environmental Science: Process and Impacts”

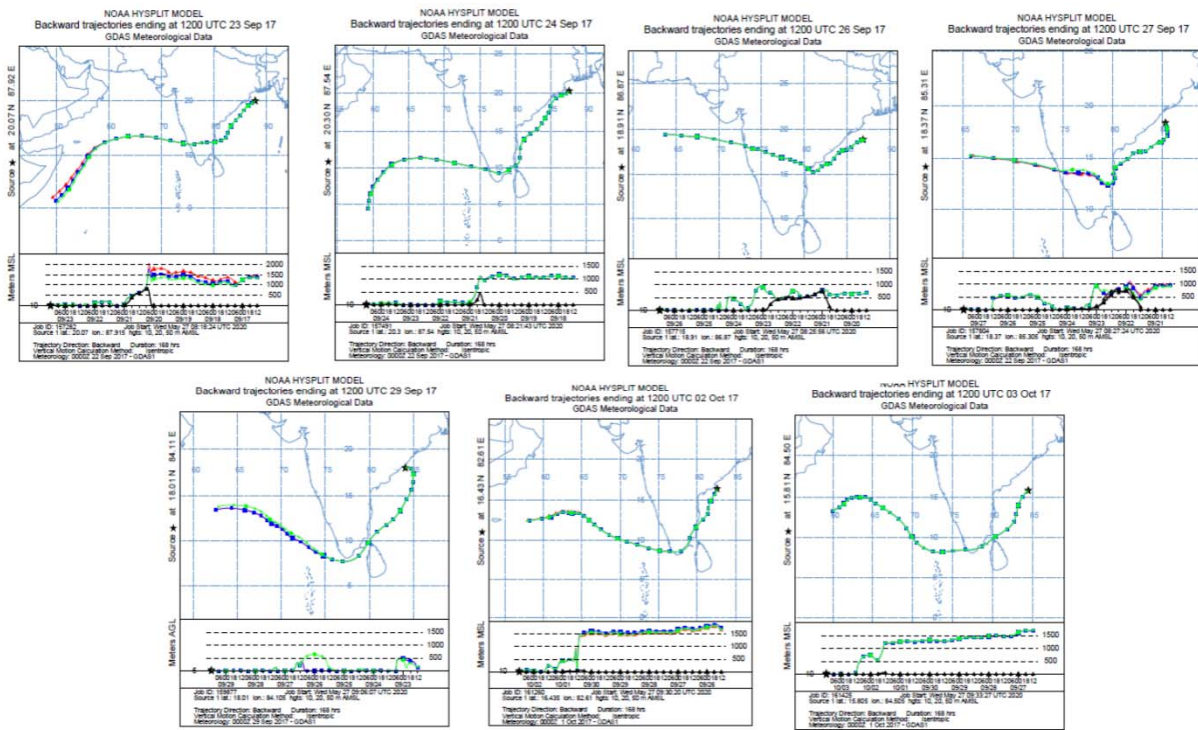


Figure S1: 7-day isentropic backward air mass trajectories over the BoB during SSK105 cruise (23 September – 3 October 2017).

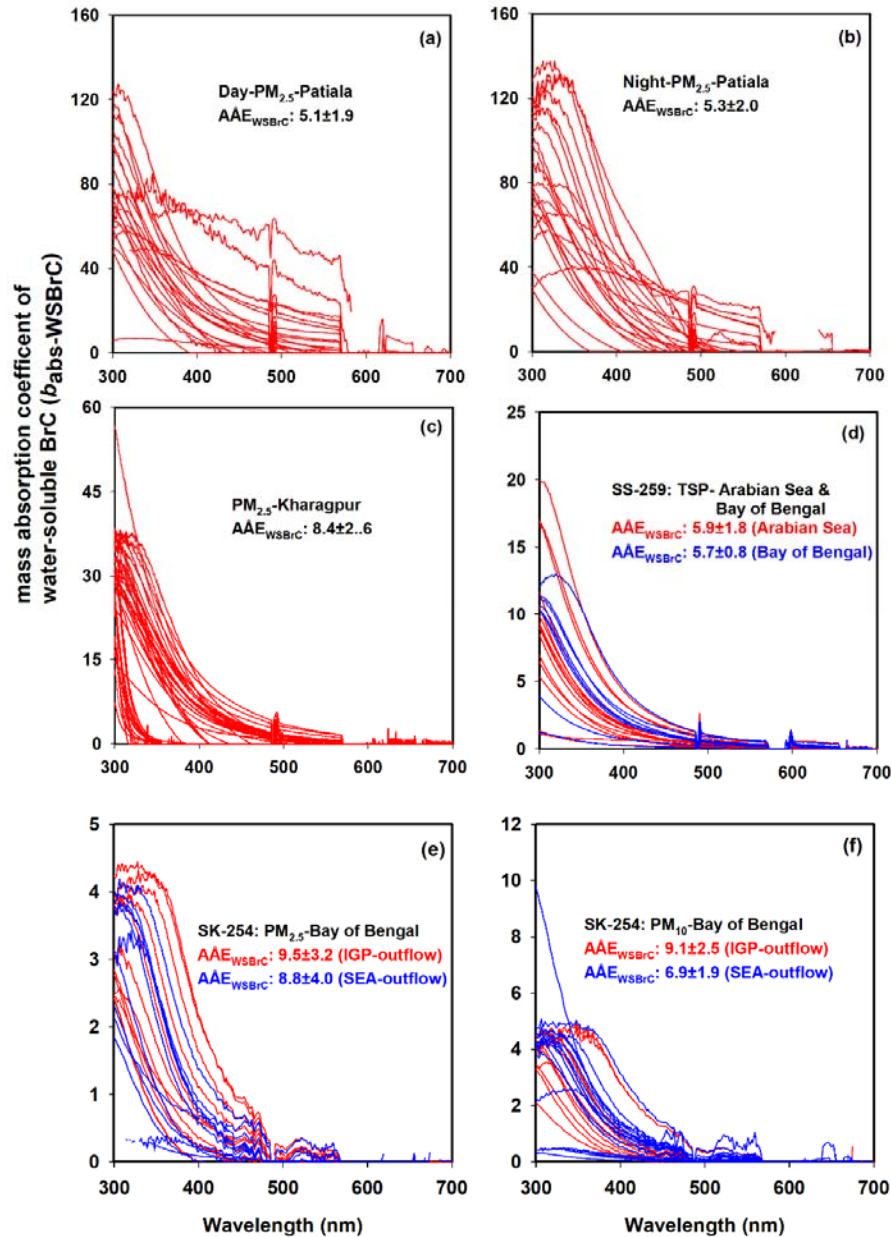


Figure S1. Typical wavelength-dependent mass absorption coefficient of water-soluble BrC ($b_{\text{abs-H}_2\text{O-BrC}}$ or $b_{\text{abs-ws-BrC}}$) in the wintertime aerosols from the Indo-Gangetic Plain (IGP) and its outflow to the Bay of Bengal, adopted from Bikkina and Sarin, ESPI, 2019¹. Here, (a-b) $b_{\text{abs-H}_2\text{O-BrC}}$ in PM_{2.5} collected over Patiala (panel. a: day time and panel. b: Night time), (c) PM_{2.5} over Kharagpur, (d) TSP Arabian Sea and Bay of Bengal during SS-259 cruise, (e and f) PM_{2.5} and PM₁₀ over the Bay of Bengal during SK-254. In Panel d, “red” and “blue” colours indicate TSP collected over the Arabian Sea and Bay of Bengal, respectively. Here, PM_{2.5} and PM₁₀ refer to particles with an aerodynamic diameter of less than 2.5 and 10, respectively. TSP is the total suspended particulate matter.

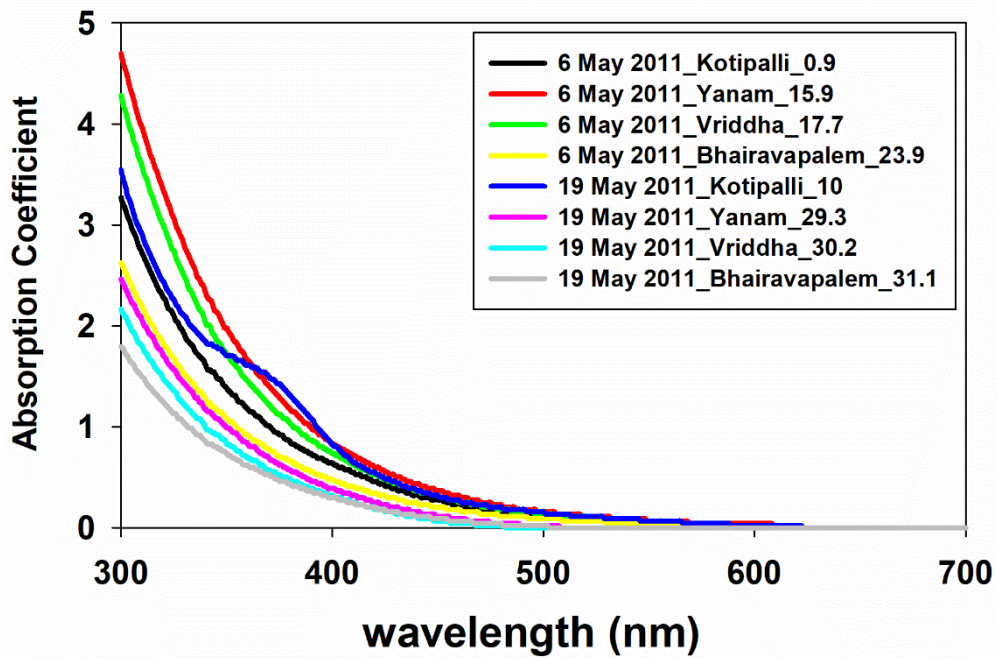


Figure S3. Absorption coefficient of colour dissolved organic matter (CDOM) measured in the surface waters collected from the Gautami-Godavari estuary draining into the Bay of Bengal during the southwest monsoon. Here, the absorption coefficient is estimated as The absorption coefficient of CDOM ($b_{\text{abs-CDOM}}$, expressed in m^{-1}) is calculated as “ $A(\lambda) \times \ln(10)/l$ ”, where $A(\lambda)$ is the absorbance at given wavelength and l is the path length of cuvette used for absorption measurement².

Table S1. Sampling details of PM₁₀ during the SSK105 cruise.

Sample codes	Start date (DD-MM-YYYY)	Start time	Starting coordinate		Stop date (DD-MM-YYYY)	Stop time	Stop coordinates		air volume (m ³)
			Lat (°N)	Lon (°E)			Lat (°N)	Lon (°E)	
23 Sept 2017	23-09-2017	6:50 AM	19.65	87.99	24-09-2017	11:00 AM	20.49	87.84	2110
24 Sept 2017	24-09-2017	1:30 PM	20.49	87.84	25-09-2017	12:00 AM	20.11	87.24	2286
25 Sept 2017	25-09-2017	12:00 AM	20.11	87.24	26-09-2017	9:30 AM	19.75	87.49	2126
26 Sept 2017	26-09-2017	12:30 PM	19.35	87.77	27-09-2017	9:30 AM	18.47	85.97	2228
27 Sept 2017	27-09-2017	1:30 PM	18.52	85.87	29-09-2017	2:00 AM	18.22	84.74	2670
29 Sept 2017	29-09-2017	9:15 AM	18.22	84.74	01-10-2017	7:50 PM	17.80	83.47	1884
2 Oct 2017	02-10-2017	12:00 PM	16.49	82.39	03-10-2017	9:00 AM	16.38	82.61	2197
3 Oct 2017	03-10-2017	1:15 PM	15.81	84.51	04-10-2017	9:00 AM	15.80	84.50	1964

Table S2. Sampling details of PM₁₀ collected over Visakhapatnam.

Sample codes	Start date (DD-MM-YYYY)	Start time	Stop date (DD-MM-YYYY)	Stop time	air volume (m ³)
16 May 2018	16-05-2018	09:59 AM	17-05-2018	10:00 AM	2391
18 May 2018	18-05-2018	09:20AM	18-05-2018	17:25 PM	808
21 May 2018	21-05-2018	18:16PM	22-05-2018	05:55 AM	1163
22 May 2018	22-05-2018	18:05 PM	23-05-2018	05:48AM	1173
24 May 2018	24-05-2018	18:06 PM	25-05-2018	05:47AM	1166
28 May 2018	28-05-2018	18:02PM	29-05-2018	05:59 AM	1195
29 May 2018	29-05-2018	17:57 PM	30-05-2018	11:50AM	1787
30 May 2018	30-05-2018	17:57 PM	31-05-2018	05:50AM	1185
4 June 2018	04-06-2018	18:15 PM	05-06-2018	05:47AM	1151

Lat: 17.72; lon: 83.22

Table S3. Monte Carlo error propagation (MCEP)-based estimates of absorption coefficient ($b_{\text{abs-H}_2\text{O}/\text{MeOH-BrC-365 nm}}$), mass absorption efficiency ($\text{MAE}_{\text{H}_2\text{O}/\text{MeOH-BrC-365nm}}$) and imaginary refractive index ($k_{\text{H}_2\text{O}/\text{MeOH-BrC-365 nm}}$) of BrC from the water and methanol extracts of PM_{10} collected over the Bay of Bengal and Visakhapatnam.

SSK105 cruise:- Monte Carlo Error Propagation (MCEP)-based BrC absorption properties												
Sampling date	$b_{\text{abs-H}_2\text{O-BrC-365 nm}}$ (Mm^{-1})		$\text{MAE}_{\text{H}_2\text{O-BrC-365 nm}}$ ($\text{m}^2 \text{g}^{-1}$)		$b_{\text{abs-MeOH-BrC-365 nm}}$ (M m^{-1})		$\text{MAE}_{\text{MeOH-BrC-365 nm}}$ ($\text{m}^2 \text{g}^{-1}$)		$k_{\text{H}_2\text{O-BrC-365 nm}}$		$k_{\text{MeOH-BrC-365 nm}}$	
	av.	sd.	av.	sd.	av.	sd.	av.	sd.	av.	sd.	av.	sd.
23-Sep-17	0.4	0.1	0.63	0.16					0.0258	0.0276		
24-Sep-17	0.56	0.13	0.61	0.16	0.44	0.45	0.07	0.018	0.0249	0.0266	0.0028	0.0031
25-Sep-17	0.3	0.07	0.34	0.09	0.11	0.11	0.015	0.004	0.0140	0.0149	0.0006	0.0007
26-Sep-17	0.12	0.03	0.16	0.04	0.29	0.29	0.038	0.01	0.0065	0.0070	0.0015	0.0017
27-Sep-17	0.4	0.1	0.63	0.17	0.36	0.36	0.049	0.013	0.0256	0.0275	0.0020	0.0022
29-Sep-17	0.51	0.12	0.63	0.17	0.22	0.22	0.03	0.008	0.0256	0.0275	0.0012	0.0013
02-Oct-17	0.39	0.09	0.54	0.14	0.28	0.28	0.037	0.01	0.0219	0.0234	0.0015	0.0016
03-Oct-17	0.98	0.23	1.48	0.39	0.18	0.18	0.029	0.008	0.0605	0.0648	0.0012	0.0013
Visakhapatnam:- Monte Carlo Error Propagation (MCEP)-based BrC absorption properties												
Sampling date	$b_{\text{abs-H}_2\text{O-BrC-365 nm}}$ (Mm^{-1})		$\text{MAE}_{\text{H}_2\text{O-BrC-365 nm}}$ ($\text{m}^2 \text{g}^{-1}$)		$b_{\text{abs-MeOH-BrC-365 nm}}$ (M m^{-1})		$\text{MAE}_{\text{MeOH-BrC-365 nm}}$ ($\text{m}^2 \text{g}^{-1}$)		$k_{\text{H}_2\text{O-BrC-365 nm}}$		$k_{\text{MeOH-BrC-365 nm}}$	
	av.	sd.	av.	sd.	av.	sd.	av.	sd.	av.	sd.	av.	sd.
16-May-18	2.73	0.65	3.10	0.81	0.13	0.14	1.44	1.44	0.3098	0.0964	0.1129	0.1212
18-May-18	2.14	0.61	1.31	0.40	0.05	0.06	1.18	1.19	0.2132	0.0563	0.0087	0.0093
21-May-18	1.32	0.26	1.48	0.33	0.06	0.06	7.38	7.45	2.8826	0.5431	0.1166	0.1222
22-May-18	1.63	0.42	1.37	0.38	0.06	0.06	1.79	1.81	0.3392	0.0846	0.0137	0.0146
24-May-18	2.02	0.45	1.50	0.37	0.06	0.06	0.98	0.99	0.1742	0.0415	0.0071	0.0075
28-May-18	1.81	0.44	1.46	0.39	0.06	0.06	2.23	2.26	0.4499	0.1228	0.0182	0.0197
29-May-18	4.31	1.01	3.23	0.83	0.13	0.14	2.03	2.05	0.5777	0.1570	0.0236	0.0253
30-May-18	1.84	0.44	1.80	0.47	0.07	0.08	7.08	7.15	2.7751	0.7425	0.1133	0.1211
04-Jun-18	2.41	0.64	1.11	0.32	0.05	0.05	4.64	4.69	0.4812	0.1319	0.0196	0.0211

References

1. S. Bikkina and M. Sarin, Brown Carbon in the continental outflow to the North Indian Ocean, *Environmental Science: Processes & Impacts*, 2019, doi: 10.1039/C9EM00089E.
2. S. R. Pandi, R. Kiran, N. S. Sarma, A. S. Srikanth, V. V. S. S. Sarma, M. S. Krishna, D. Bandyopadhyay, V. R. Prasad, T. Acharyya and K. G. Reddy, Contrasting phytoplankton community structure and associated light absorption characteristics of the western Bay of Bengal, *Ocean Dynamics*, 2014, **64**, 89-101.